UNIVERSITÀ DEGLI STUDI DI SASSARI

SCUOLA DI DOTTORATO IN
SCIENZE VETERINARIE

INDIRIZZO: **Patologia e Clinica Animale (XXVII CICLO)**

Use of Two-Dimensional Speckle Tracking Echocardiography to Assess Left Ventricular Systolic Function in Dogs with Systemic Inflammatory Response Syndrome

Docente Guida
Prof.ssa Maria Luisa Pinna Parpaglia

Direttore
Prof. Sergio Ledda

Tesi di Dottorato del
Dott. Andrea Corda

ANNO ACCADEMICO 2014 – 2015

Unione europea
Fondo sociale europeo

REPUBBLICA ITALIANA

REGIONE AUTÒNOMA DE SARDIGNA
REGIONE AUTONOMA DELLA SARDEGNA

FSE 2007-2013
POR SARDEGNA
obiettivo competitività regionale e occupazione

UNIVERSITÀ DEGLI STUDI DI SASSARI

SCUOLA DI DOTTORATO IN
SCIENZE VETERINARIE

INDIRIZZO: **Patologia e Clinica Animale (XXVII CICLO)**

Use of Two-Dimensional Speckle Tracking Echocardiography to Assess Left Ventricular Systolic Function in Dogs with Systemic Inflammatory Response Syndrome

Docente Guida

Prof.ssa Maria Luisa Pinna Parpaglia

Direttore

Prof. Sergio Ledda

Tesi di Dottorato del

Dott. Andrea Corda

ANNO ACCADEMICO 2014 – 2015

La presente tesi è stata prodotta nell'ambito della Scuola di Dottorato in "Scienze Veterinarie" dell'Università degli Studi di Sassari, a.a. 2014/2015 – XXVII ciclo, con il supporto di una borsa di studio finanziata con le risorse del P.O.R. SARDEGNA F.S.E. 2007-2013 - Obiettivo competitività regionale e occupazione, Asse IV Capitale umano, Linea di Attività l.3.1.

Acknowledgements

A very special thanks goes to Prof. Anne French from the Small Animal Hospital, University of Glasgow, Prof. Pablo Gomez Ochoa from the Department of Animal Pathology, University of Zaragoza and Prof.ssa Maria Luisa Pinna Parpaglia from the Department of Veterinary Medicine, University of Sassari for giving me their valuable teachings and suggestions during the last four years. My research would not have been possible without their helps.

Of course I would like to give particular thanks to Maurizio Chiodi and Massimiliano Porretta, from Esaote company, for giving me the technical support during the study,

I would also like to acknowledge Prof. Giovanni Sotgiu, from the Department of Biomedical Science, University of Sassari, for providing the statistical analysis and Dott.ssa Rosanna Zobba, from the Departement of Veterinary Medicine of the University of Sassari, for the laboratory support.

Moreover I want to express my sincere thanks to the University of Sassari and in particular to the Department of Veterinary Medicine for giving me the chance to make the great experience of the European PhD during which I had the opportunity to grow professionally and the fortune to meet many wonderful colleagues and friends from all over Europe.

I want to thanks my parents, my sisters and my aunts Franca and Peppina for being such a huge support through my education and my experiences.

Last, but certainly not least, I'd like to thanks Marzia for her love, support, encouragement and patience during my pursuit of the European Doctorate in Veterinary Science.

Andrea

Table of contents

LIST OF ABBREVIATIONS 3
ABSTRACT 4

1. INTRODUCTION 5
1.1 SIRS 5
1.2 PATHOPHYSIOLOGY OF SIRS 6
1.3 PATHOPHYSIOLOGY OF MODS 10
1.4 MYOCARDIAL DEPRESSION IN SIRS 12
1.4.1 Cardiac myocyte contraction 12
1.4.2 Pathophysiology of myocardial depression in SIRS and sepsis 14
1.4.3 Myocardial injury in SIRS 18
1.4.4 Myocardial dysfunction in SIRS 19
1.5 ADVANCED TECHNIQUES IN VETERINARY ECHOCARDIOGRAPHY 24

2. OBJECTIVE OF THE STUDY 34

3. MATERIALS AND METHODS 36
3.1 CASE SELECTION 36
3.1.1 SIRS group 36
3.1.2 Control group 37
3.2 DATA COLLECTION 38
3.2.1 Blood collection 38
3.2.2 Echocardiographic examination 39
3.2.3 Two-dimensional Speckle Tracking Echocardiography 41
3.3 VARIABILITY STUDY 44
3.4 STATISTICAL ANALYSIS 45

4. RESULTS 46
4.1 SIGNALMENT 49
4.2 MEAN CRP, CTNI AND HEART RATE 49
4.3 2D, M-MODE AND DOPPLER DERIVED INDICES OF LV SYSTOLIC FUNCTION 50
4.4 MEAN EF% OBTAINED BY SPECKLE TRACKING METHOD 53
4.5 SPECKLE TRACKING ENDOCARDIAL VARIABLES 54
4.6 SPECKLE TRACKING EPICARDIAL VARIABLES 56
4.7 SPECKLE TRACKING TRANSVERSAL STRAIN AND STRAIN RATE VARIABLES 57
4.8 VARIABILITY STUDY 58
4.9 CORRELATION BETWEEN VARIABLES 58

5. DISCUSSION 63

6. CONCLUSIONS 68

REFERENCES 69

List of abbreviations

2Ch	Two Chambers
2D	Two-Dimensional Echocardiography
2D STE	Two-Dimensional Speckle Tracking Echocardiography
3Ch	Three Chambers
3D	Three Dimensional
4Ch	Four Chambers
AFI	Automated Function Imaging
APPs	Acute Phase Proteins
AT	Antithrombin
ATP	Adenosine Triphosphate
BP	Blood Pressure
CBC	Cell Blood Count
CI	Cardiac Index
CO	Cardiac Output
COX-2	Cyclooxygenase 2
CPV	Canine Parvovirus
CRP	C-reactive Protein
CV	Coefficient of Variation
cTn	Cardiac Troponin
cTnI	Cardiac Troponin I
DAMP	Damage Associated Molecular Pattern
DCM	Dilated Cardiomyopathy
DNA	Deoxyribonucleic Acid
DO	Oxygen Delivery
ECG	Electrocardiogram
ECM	Extracellular Matrix
ECVIM-CA	European College of Veterinary Internal Medicine-Companion Animals
EF	Ejection fraction
ENDO	Endocardial Border or Endomyocardium
EPI	Epicardial Border or Epimyocardium
EPSS	E-point to Septal Separation
ESVI	End Systolic Volume Index
ET	Ejection Time
ET1	Endothelin-1
ETC	Electron Transport Chain
FPS	Frames per Second
FR	Frame Rate
FS	Fractional Shortening
GLPS	Global Longitudinal Peak Strain
HMGBP1	High Mobility Group Box Protein 1
HR	Heart Rate
IBD	Intestinal Bowel Disease
IL	Interleukin
IL-1	Interleukin One
IL-6	Interleukin Six
IMP	Index of Myocardial Performance
iNOS	Nitric Oxide Synthase
IVS	Interventricular Septum
LA	Left Atrium

LiDCO	Lithium Dilution Cardiac Output
LPS	Lipopolysaccharide
LTCC	L-type Calcium Channels
LV	Left Ventricle
LVDV	Left Ventricular Diastolic Volume
LVGLS	Left Ventricular Global Longitudinal Strain
LVSV	Left Ventricular Systolic Volume
LVIDd	Left Ventricular Internal Diameter in Diastole
LVIDs	Left Ventricular Internal Diameter in Systole
LVPW	Left Ventricular Posterior Wall
MDS	Myocardial Depressant Factor
MODS	Multiple Organ Dysfunction Syndrome
MOF	Multiple Organ Failure
MRI	Magnetic Resonance Imaging
NF-κB	Nuclear Factor Kappa B
NK	Natural Killer
NO	Nitric Oxide
PAF	Platelet-Activating Factor
PAMPS	Pathogen Associated Molecular Pattern
PCO_2	Partial Pressure of Carbon Dioxide
PEP	Pre Ejection Period
PMNLs	Polymorphonuclear Leukocytes
PRR	Pattern Recognition Receptor
PW	Pulsed Wave Doppler
RA	Right Atrium
RBCs	Red Blood Cells
RV	Right Ventricle
RyR	Ryanodine Receptors
SD	Standard Deviation
SERCA	Sarcoendoplasmic Reticulum Ca^{2+}-ATPase
SIRS	Systemic Inflammatory Response Syndrome
SMOD	Simpson's Method of Disks
SR	Sarcoplasmic Reticulum
St	Strain
STE	Speckle Tracking Echocardiography
StR	Strain Rate
TDI	Tissue Doppler Imaging
TF	Tissue Factor
TLR	Tool Like Receptor
TM	Thrombomodulin
TnC	Troponin-C
TNF	Tumour Necrosis Factor
TNF- α	Tumour Necrosis Factor Alpha
TnI	Troponin-I
TnT	Troponin-T
WBC	White blood cell

Abstract

SIRS is a clinical syndrome caused by systemic inflammation of infectious or non-infectious origin. SIRS is characterized by an endogenous cascade of interleukins and others inflammatory mediators such as TNF-α IL-6 and IL-1 which are responsible to the myocardial depression during systemic inflammation. Conventional echocardiographic indices of LV systolic function such as Fractional Shortening (FS%) and Ejection Fraction (EF%) are not sensitive enough to detect mild or early systolic dysfunction in dogs suffering from SIRS. Speckle-Tracking Echocardiography (STE) is a new echocardiographic technique that allows an objective and quantitative evaluation of global and regional myocardial function through the analysis of the motion of speckles that are created by the interaction of ultrasonic beams and the myocardium during the 2D exam. In the present study we tested the hypothesis that 2D-STE may detect LV systolic dysfunction, not diagnosed by conventional echocardiography, in dogs with SIRS. 17 dogs with evidence of SIRS and 17 healthy dogs as a control group were included in this prospective study. At the time of Veterinary Teaching Hospital admission each dog was submitted to standard 2D, M-mode, Doppler and 2D Speckle Tracking echocardiography to assess systolic function. Furthermore, blood samples were obtained for the measurements of cTnI and CRP serum levels. To assess the intraobserver within-day and between-day variability of the 2D-STE acquisition and measurements we performed a study of variability on 5 healthy dogs belonging to the control group. The results showed that the 2D-STE had low intraobserver variability and that the LV Global Longitudinal Peak Strain of endomyocardial layer (ENDO GLPS) and the STE-derived Ejection Fraction (EF%) were lower in the SIRS group than in the control group. On the contrary, standard 2D and M-Mode indices of systolic function such as EF%, FS% weren't significantly different between the two groups. We didn't find significant correlation between CRP serum levels and 2D-STE variables and between cTnI and ENDO GLPS. Our study demonstrated that 2D-STE was more sensitive than standard echocardiography in detecting early or mild to moderate myocardial dysfunction, not detected by conventional echocardiography, in a population of dogs with SIRS.

1. INTRODUCTION

1.1 SIRS

The *Systemic Inflammatory Response Syndrome (SIRS)* is a clinical syndrome caused by systemic inflammation of infectious or non-infectious origin. The term SIRS was introduced by the American College of Chest Physician and Society of Critical Care Medicine Consensus Conference held in Chicago in August 1991. The committee defined SIRS as a complex pathophysiologic response to a variety of insults such as infection, pancreatitis, ischemia, multiple trauma, tissue injury, haemorrhagic shock, immune-mediated organ injury and the exogenous administration of inflammatory mediators such as Tumour Necrosis Factor (TNF) and other cytokines[1]. Sepsis was defined as a systemic inflammatory response to infection. The pathophysiologic state of the SIRS has been studied extensively. The onset of inflammation results in a complex set of interactions within the immune system to minimize injury and preserve organ function. A contained inflammatory response can become over-exuberant and deregulated by on-going injury, the addition of new insults or a compromised immune system. An uncontrolled generalized activation of the inflammatory reaction in organs remote from the initial insult can progress to secondary multiple organ dysfunction syndrome[1] (MODS), multiple organ failure (MOF) and death[2]. Heart rate, respiratory rate, body temperature and white blood cell count are the clinical criteria used to categorize patients with SIRS in veterinary[3] and human medicine[1]. SIRS criteria have been used to determine the severity of illness and prognosis in critically ill dogs[3] and in puppies with canine parvovirus infection[4] in both studies mortality was significantly associated with the number of criteria fulfilled. In the field of canine medicine, SIRS has been described in a lot infectious and non infectious clinical conditions such as bite wound trauma[2], soft tissue trauma, gastrointestinal foreign body/obstruction, gastrointestinal ulceration, septic peritonitis, parvovirus enteritis, mast cell tumour, lymphoma, pancreatitis, pancreatic adenocarcinoma and pyelonephritis[5] as well as in immune mediated haemolytic anaemia, fever of unknown origin[6], mammary

tumour, splenic haemangiosarcoma, gastric volvulus, canine distemper virus infection, leptospirosis[7], urinary tract infections, pneumonia, polyarthitis[8], staphylococcal skin infection[9], subcutaneous infections, hepatobiliary bacterial infections[10] splenic torsion, bile peritonitis, heat stroke[11], babesiosis[12], uterine infections, prostatitis, osteomyelitis, abscesses[13], discospondylitis, myositis, steroid-responsive meningoencephalitis, prostatic abscess, mastitis and pulmonary carcinoma[14]. Differentiating between sepsis and non-infectious forms of SIRS can be a diagnostic challenge as the clinical presentation is often similar[10].

1.2 Pathophysiology of SIRS

SIRS and sepsis are characterized by the activation of a strong immune response. The innate immune response is the first line of defence against a microbial invader and represents a nonspecific response that can be quickly activated by innate-cell types such as neutrophils and macrophages. These cells have Pattern Recognition Receptors (PRRs) that identify different microbial molecules know as Pathogen-Associated Molecular Pattern (PAMPs). The most widely recognized PAMP is lipopolysaccharide (LPS) of Gram-negative bacteria. When a PRR recognizes a PAMP, cells of the innate immune system generate a strong response that may ultimately result in the death of the invading microorganism. This can be achieved by phagocytosis or by inducing an up regulation of the immune response by interaction with the adaptive immune system, based on a system of T and B-lymphocytes that respond to specific epitopes.

Among the membrane-bound PRRs, the Toll-Like Receptors (TLRs) are the first identified and best characterized. TLRs are highly conserved and expressed ubiquitously throughout species, including mammalian. In mammalian they are expressed in immune cells such as monocytes/macrophages, neutrophils, natural killer cells, dendritic cells, mast cells, specific T and B lymphocytes and non immune cells such as epithelial cells, skin keratinocytes, fibroblasts, cardiomyocytes and endothelial cells in the heart[15]. The TLRs are able to recognize and respond to a large number of microbial organisms including Gram-

negative and Gram-positive bacteria, Mycoplasma spp., fungi, viruses, parasites, bacterial flagellin as well as host cells colonized by viral pathogens. In addition to microbial PAMPs, TLRs can recognize endogenously produced mediators that are released in response to injury or inflammation called Damage-Associated Molecular Patterns (DAMPs). DAMPs are endogenous molecules specifically generated upon tissue injury. Some are intracellular molecules normally inaccessible to the immune system that are released into the extracellular milieu as a result of cell necrosis or activation following injury. Others are extracellular matrix (ECM) molecule fragments that are released upon tissue damage or ECM molecules that are specifically up regulated in response to tissue injury. DAMPs are vital danger signals that alert the immune system to tissue damage upon both infectious and sterile insult. DAMPs have implicated in diseases where excessive inflammation plays a key role in pathogenesis, including autoimmune disease and cancer[16]. PAMPs and/or DAMPs identification by TLRs leads a complex cascade of intracellular signals that culminates in the activation of the transcriptional factor "Nuclear Factor kappa B" (NF-κB) leading inflammatory gene expression[17]. NF-κB activates transcription sites for a variety of genes including pro-inflammatory cytokines, chemokines, and other inflammatory mediators such as Tumour Necrosis Factor alpha (TNF-α), Interleukins (ILs) 1, 6, 8, 12 and Interferon (IFN-α and INF-β)[18]. Cytokines are soluble proteins produced and secreted as part of the immune response to a variety of insults including infection, cancer, and autoimmunity. Chemokines are similar proteins, but they induce chemotaxis and promote the migration of certain cells to areas of infection[18]. Cells of the immune system secrete most of these pro-inflammatory mediators. The primary function of these molecules is to promote inflammation by signalling pathways that induce expression of inflammatory products, which have direct effects on the host vasculature and facilitate the transmigration of leukocytes to the site of infection. Dogs with SIRS of infectious or non-infectious origin demonstrate high levels of interleukins in their bloodstream[14, 19, 20].

TNF-α is predominantly produced by activated macrophages and T-cells but also by mast cells, B-cells, Natural Killer (NK) cells, neutrophils, endothelial cells, myocytes, osteoblasts and fibroblasts. Many of the classical features of inflammation can be attributed to the actions of TNF-α upon the endothelium with increased production of Nitric Oxide Synthase (iNOS) and Prostaglandin Synthase type 2 (cyclooxygenase 2 or COX-2) leading to vasodilatation and local slowing of blood flow. TNF-α also stimulates the expression of endothelial adhesion molecules that lead to the tethering of leukocytes to the endothelial wall and their transmigration into the interstitium accompanied by fluid and plasma macromolecules. In addition to the up-regulation of iNOS, COX-2 and adhesion molecules, TNF-α also induces the expression of pro-coagulant proteins such as Tissue Factor (TF) and down regulates anti-coagulant factors such as Anti-thrombin (AT) and Thrombomodulin (TM), leading to the activation of coagulation cascade[21]. Monocytes and endothelial cells are the predominant cell type to express Tissue Factor after appropriate stimulation by endotoxin, immune complexes, cytokines (TNF-α and IL-6), and activated platelets[22]. Increased serum activity of TNF-α correlate strongly with a severe outcome or mortality in canine parvovirus infection[23] and acute pancreatitis[24]. Another important pro-inflammatory cytokine in SIRS is the **interleukin-6,** it is a powerful pyrogen and it has a strong stimulatory effect upon leukocyte activation and myeloid progenitor cell proliferation[25]. Many papers report increase of serum concentration of IL-6 in SIRS and sepsis dogs. Rau et al reported that plasma IL-6 concentration is predictive of outcome in naturally occurring canine SIRS and sepsis[14]. Do-Hyeon et al found high IL-6 plasma levels in dogs with infectious and non-infectious SIRS, in the same study IL-6 levels were not related to outcome[19]. Increased TNF-α and IL-6 serum concentration in dogs has been reported in a canine model of sepsis induced by endotoxin[26] and in a group of 45 dogs with natural occurring SIRS (22 with sepsis and 23 with non infectious SIRS). In the last report mentioned above TNF activity and IL-6 concentration were not different in dogs with sepsis compared to dogs with non-infectious

SIRS and authors didn't find correlation between TNF bioactivity, IL-6 concentration and survival to discharge[27]. TNF-α and IL-6 are both known for inducing the expression of pro-coagulant proteins such as Tissue Factor (TF). **Interleukin-1 (IL-1)** acts like TNF-α in the hyper acute period after immune stimulation in sepsis and SIRS. It induces the synthesis of adhesion molecules and cytokines by endothelial cells, stimulates leukocyte activation and endothelial tethering and transmigration into the interstitium. IL-1 also up regulates iNOS and COX2 production, acts as the mayor endogenous pyrogen in fever, and increases corticosteroid release via hypothalamic effects[21]. Recently another cytokine has been identified as being critical in dogs with SIRS and sepsis, it is the High Mobility Group Box Protein 1 (HMGBP1), an endogenous protein released into the circulation after necrotic or apoptotic cell death, it has direct pro-inflammatory actions. Dogs with SIRS and high plasma levels of HMGBP1 were associated with worse outcome regardless of the aetiology of SIRS[19,28]. Under normal circumstances, cytokines exert their actions locally and their effects are restricted to neighbouring cells. Although their local effects benefit the host since they are designed to limit the initial injury or infection, in cases of severe inflammation or infection, the excessive release of pro-inflammatory cytokines overwhelms the host's compensatory anti-inflammatory response and results in progressive endothelial dysfunction, increased microvascular permeability and activation of the coagulation system[7, 29–31]. During systemic inflammation, the pro-inflammatory cytokines stimulate the synthesis and the release of large quantities of acute phase proteins (APPs) from hepatocytes and other cells. For years APPs were thought to be synthetized only by the liver, however, there is growing evidence that they also can be produced in other organs such as kidney, intestine, heart, and different types of white blood cells in humans[32,33]. APPs have a variety of functions designed to re-establish homeostasis, assisting in pathogen elimination and overcoming inflammation. The acute phase response is characterized by fever, neutrophilia, activation of the coagulation and complement cascades, serum iron and zinc binding, enhanced

gluconeogenesis, increased muscle catabolism, and altered lipid metabolism[34]. As a consequence of the up-regulation of APPs production, concentrations of other plasma proteins such as Albumin, Protein C, Antithrombin (AT) and Protein S (collectively know as negative APPs)[35, 36] decrease. A number of APPs have been characterized in veterinary species[37] including dogs[38], and they have been used as biomarkers of systemic inflammation in both research and clinical practice[39]. C-Reactive Protein (CRP) is a major APP in dogs. The normal levels and the effect of age and sex on the CRP concentration in healthy dogs has been investigated and no correlation has been observed[40, 41]. CRP increase rapidly after a systemic inflammatory stimulus triggered by various clinical conditions[42–45] such as infection[46–49], neoplasia[50–52], trauma[43], immune-mediated diseases[53, 54] parasites[55–57] and other inflammatory states like acute pancreatitis[58] and snake envenomation[59]. Interestingly, several studies have reported raised serum levels of CRP in pregnant bitches[39, 40, 60] from day 21 to day 55 after ovulation. Probably, the endometrial injury caused by the implantation itself provokes this response in the maternal circulation. In general, serum CRP concentration provides a sensitive but nonspecific means of measuring inflammation. A recent study of SIRS and sepsis in dogs demonstrated a correlation between decreasing serum CRP concentration and recovery from disease, suggesting its use as a prognostic biomarker in this context[61].

1.3 Pathophysiology of MODS

MODS defines the progressive, but potentially reversible, dysfunction of two or more organ systems after acute life-threatening disruption of systemic homeostasis[62]. Organ systems that can be affected in patients with MODS include the renal, cardiovascular, respiratory, hepatic, hematologic, neurologic, gastrointestinal, endocrine and immune systems[63]. Mortality rates increase as the number of dysfunctional organ systems increase. A veterinary clinical report in 2010, of 114 dogs with sepsis secondary to gastrointestinal tract leakage, found that the overall mortality rate was 70% with MODS and 25% for those with only

dysfunction of one organ system. In this study the risk of death increased as the number of dysfunctional organs increased, and dysfunction of either the respiratory, cardiovascular, renal or coagulation system was independently associated with a significantly increased odds of death[64]. The exact pathophysiology of the development of MODS has not been completely defined. It is likely that multiple pathophysiologic mechanisms and mediators are involved in the pathogenesis of this injury process. A number of the potential pathophysiologic mechanisms, which may act individually or collectively in the production of organ system dysfunction, are:

- **Collateral tissue damage** caused by activated immune cells[65] and the direct toxicity (cytopathic changes consequent to cytokine-cell receptor interactions) of the systemically released mediators of the SIRS response.
- **Inadequate tissue perfusion** or the misdistribution of blood flow, which contains oxygen, nutrients, and other important substrates required to support cellular and organ function. In the setting of sepsis and SIRS there is commonly a decrease in the cardiac output, decreased systemic perfusion pressure which may result in hypoperfusion or ischemia of the organ system. The period of ischemia may be followed by reperfusion and oxidative injury, which may produce organ system dysfunction/failure. Tissue ischemia also may result from the aggregation of microthrombi composed of platelets, PMNLs, RBCs, and fibrin, which may obstruct the small capillaries and impair the delivery of blood and substrate to the tissues.

Some authors have speculated that even though adequate blood flow may reach the various tissue beds, there may be an inability of the mitochondria or cells to take up or use the delivered oxygen and substrate. The inflammatory cytokines IL-1β and TNFα promote mitochondrial oxidant production thus increase the state of oxidative stress[66]. Strong evidence suggests that oxidative stress may be responsible for mitochondrial damage during sepsis and other acute illnesses.

The free radicals can damage mitochondrial proteins, including components of the Electron Transport Chain (ETC) [67] and mitochondrial DNA [68]. Mitochondria damage results in impaired oxygen utilization and attendant reduction in the capacity to produce ATP, which is associated with loss of cellular function in vital organs[69].

1.4 Myocardial depression in SIRS

1.4.1 Cardiac myocyte contraction

Before describing the pathophysiological mechanisms that are assumed to be responsible for the myocardial depression in sepsis and SIRS, it is appropriate to describe briefly the physiology of myocardial contraction. Cardiac myocytes are a type of striated muscle cells, so called because cross striation are observed microscopically. Myocytes connect to each other by way of specialized cell membranes called intercalated disk forming a branching network of cells that is sometimes referred to a functional syncytium. Within the intercellular regions there are gap junctions, which permit cell-to-cell conduction of electrical currents. Gap junction ensure that the electrical impulse travel to all the interconnected myocytes allowing the myocardium to contract as a unit. The functional unit of the myocyte is the sarcomere, composed of thick and thin filaments. Thick filaments are composed of myosin, whereas thin filaments contain actin and other associated proteins [70].

Myocardial contraction and relaxation are regulated by the interaction among contractile proteins (actin and myosin filaments), regulatory proteins (troponin and tropomyosin) and calcium ions. About 300 molecules of myosin packed together compose each thick filament and six thin filaments surround it. Each thin filament is composed of actin, tropomyosin and troponin. Actin is a globular protein arranged as a chain of repeating globular units, forming two helical filaments. Interdigitated between the actin filaments there are regulatory proteins called tropomyosin. Each tropomyosin molecule is associated with seven actin molecules. Attached to the tropomyosin at regular intervals there is the troponin regulatory complex, made up of three subunits: Troponin-T (TnT), which

attaches to the tropomyosin; Troponin-C (TnC), which serves as a binding site for Ca^{2+} during excitation-contraction coupling and Troponin-I (TnI), which binds to actin. In the resting state, tropomyosin blocks the site of actin–myosin interaction, while the TnI subunit inhibits the actin–myosin ATPase. Following the myocyte depolarization, during phase 2 of the cardiac action potential, extracellular Ca^{2+} enters the myocyte through sarcolemmal L-type Calcium Channels (LTCC) also known as the Dihydropyridine Channels. This, in turn, lead to release of intracellular Ca^{2+}, stored in the Sarcoplasmic Reticulum (SR) via Ryanodine Receptors (RyR). As the intracellular Ca^{2+} concentration increases, the ion binds the TnC in a concentration dependent manner. This leads to conformational changes in the troponin-tropomyosin regulatory complex, which move away from the myosin-binding site on the actin molecule. Actin and myosin are then free to crosslink and contraction proceeds with ATP hydrolysis. Ca^{2+} channel closure at the end of phase 2 of the action potential prevents extracellular influx, while the Sarcoendoplasmic Reticulum Ca^{2+} ATPase (SERCA) pumps cytoplasmic Ca^{2+} back into the SR. Calcium is also returned extracellularly via the sodium-calcium exchanger. As intracellular Ca^{2+} concentration declines, troponin-tropomyosin complex reassumes its inhibitory configuration, and myocardial relaxation starts. ATP is required both for providing the energy for contraction and for relaxation. In the absence of sufficient ATP as occurs during cellular hypoxia, cardiac muscle contraction and relaxation will be impaired. Sarcoplasmic Ca^{2+} concentration determines the force of myocardial contraction. Higher intracellular levels lead to greater relief of troponin-tropomyosin complex inhibition, rendering more actin-myosin complexes active. β-adrenergic stimulation augments cardiac contractility by increasing intracellular Ca^{2+} influx, therefore, noradrenaline (released by sympathetic nerves) and adrenaline (released by the adrenal glands) are positive inotropic agents; β-agonism also promotes myocyte relaxation enhancing SERCA activity and preserving diastolic function. Cholinergic stimulation, in turn, decreases contractility by down regulating intracellular Ca^{2+} influx. This

pathway is coupled to Muscarinic Receptors (M_2) that bind acetylcholine released by parasympathetic (vagal) nerves within the heart, therefore, acetylcholine is a negative inotropic agent[70].

1.4.2 Pathophysiology of myocardial depression in SIRS and sepsis

Myocardial depression is a major contributor to mortality and morbidity in human patients with sepsis, in fact, in the 40% of patients who experience myocardial dysfunction as a complication of sepsis, the mortality rises from 70% to 90%[71]. In human medicine contractile dysfunction in the septic patients is defined as biventricular dilatation, reversible decrease in ejection fraction, diminished blood pressure response to intravenous fluids, and reduced ability to augment cardiac output despite increased levels of circulating catecholamines [72].
Cardiac function is severely impaired in sepsis, severe SIRS[73] and MODS[74]. Although there are numerous causes of SIRS, sepsis is the most investigated, essentially because it is a leading cause of death in critically ill patients. Nevertheless, septic myocardial impairment remains a clinical enigma.
Wiggers in 1947 postulated the presence of a circulating myocardial depressant factor (MDF) in some cases of human shock[75]. Waisbren in 1951 was the first to report myocardial dysfunction in patients with sepsis, and subsequent experimental studies were able to confirm the suspected myocardial depressant factor in sepsis[76]. In 1985 Parrillo and colleagues[77] demonstrated that serum of septic patients generated concentration-dependent depression of in vitro myocyte contractility. This was the first study that confirmed the long suspected link between sepsis and a circulating myocardial depressant factor. Using hemofiltration techniques, researchers found that the stimulating factor was greater than 10 kDa, heat labile, and water soluble, suggesting a protein or polypeptide[78]. Lipopolysaccharide (LPS) was postulated to represent the MDS because its infusion in animals and humans produced the hyperdynamic, hypotensive state seen in naturally occurring septic shock[78]. A second hypothesis suggested that reduced myocardial perfusion, due to peripheral vasodilation and hypotension, was involved in septic myocardial depression[79]. However, clinical

studies[80] evidenced that coronary perfusion during septic shock was preserved or even increased and that hypotension was more likely the product of profound reduction in systemic vascular resistance.

Although endotoxin was sufficient to produce septic shock, it was unlikely to explain the complete mechanism in itself. Experimental studies found that gram-positive bacteria produced the same pattern of cardiovascular changes as those invoked by endotoxin[81]. Furthermore, many patients that were culture negative or had no detectable levels of endotoxemia manifested the typical cardiovascular modifications of patients with septic shock. These findings suggested that endotoxin, and several other molecules contributed to the activation of an endogenous cascade of local and systemic inflammatory mediators, which caused myocardial dysfunction in sepsis and SIRS. Nowadays, researchers around the world believe that cytokines such as TNF-α, IL-6 and IL-1 are the main causes of the myocardial depression in SIRS/sepsis. In vitro studies showed significant decreases in measures of contractility in cardiomyocytes exposed to TNF-α, IL-1β [82], and IL-6 [83].

The cellular mechanisms underlying cytokine-mediated cardiomyopathy have been extensively studied but remain incompletely elucidated. Alteration of intracellular calcium currents, overproduction of Nitric Oxide (NO), Endothelin-1 (ET1) and Platelet-Activating Factor (PAF), oxidation–reduction imbalance, altered mitochondrial activities, autonomic deregulation, microcirculatory alterations and changes in load conditions, have all been invoked in explanation.

a) Lew et al in 1996 reported a reduction in cardiac Dihydropyridine Receptors (LTCC) by 25% during induced endotoxemia in rabbits[84]. Zhong et al reached the same conclusions by performing an experimental study on ventricular myocytes from endotoxemic guinea pigs[85]. Since Dihydropyridine Receptors are primarily L-type Calcium Channels (LTCC), their reduction in endotoxemia may contribute to reduce intracellular Ca^{2+} influx during the action potential resulting in negative inotropic effect. Rigby et al in 1998, strengthened this hypothesis by

showing that decreased available Ca^{2+}, rather than decreased myofilament Ca^{2+} responsiveness, led to decreased contractile function of the pig heart during endotoxemia[86]. Finally, Stengl et al in 2010 demonstrated that septic shock, in pigs, was associated with decreased number of functional LTCC and reduction of myocyte Ca^{2+} influx. As a consequence of the decreased L-type Calcium current there was a shortening of cardiac repolarization[87].

b) TNF-α and IL-1 induce iNOS up-regulation during inflammatory response. The role of NO is well recognized in SIRS and sepsis. NO has a direct effect on cardiomyocytes, probably inducing contractile dysfunction[82]. NO inhibits mitochondrial function in various organs, including the heart. The underlying mechanisms of mitochondrial dysfunction induced by NO are still incompletely elucidated. The NO overproduction can cause direct oxidative damage and inhibition of oxidative phosphorylation complexes. As a consequence, mitochondrial ATP generation is compromised, and energy depletion may contribute to cardiac contractile dysfunction. It further induced vasodilation with resulting changes in load conditions (preload and afterload) and myocardial perfusion.
c) Persistently elevated ET-1 plasma levels are associated with myocardial dysfunction in sepsis[88] but the exact role of ET-1 in the pathogenesis of myocardial depression in sepsis is not completely understood. ET-1 may have a direct myocardial depressive action. It also produces deregulation of systemic and regional vascular tone and itself may trigger increased inflammatory cytokines and NO[89].
d) Prostanoids, including thromboxane and prostacyclin, may contribute to impaired cardiac function by altering coronary endothelial function and promoting intracoronary leukocyte activation[90].
e) Platelet-Activating Factor has been reported to directly decrease myocardial contractility via a specific, high-affinity cardiac PAF receptor.

PAF directly decreases velocity of contraction, and of relaxation in cardiomyocytes[91].

f) Autonomic impairment, identified experimentally following endotoxin exposure, could be related to alterations within the brain, the autonomic nervous system, or the pacemaker cell itself[73]. The autonomic deregulation includes resistance to catecholamines, despite elevated circulating levels of these mediators in SIRS/sepsis. The effect is mediated by decreased density or dysfunction of myocardial adrenoreceptors[92]. Studies have identified that endotoxin-induced alterations of heart rate variability are mediated, at least in part, by direct interaction with the cardiac pacemaker cells[93].

g) Changes in loading condition are common in SIRS. Cytokines increase capillary permeability leading to decreased intravascular volume (reduced preload). The release of vasodilating factors like NO, TNF-α and prostaglandins, and the vascular decreased response to vasopressor agents leads to a reduction in afterload and hypotension.

h) Microcirculatory alterations are pathological changes in the capillary bed related to microtrombi formation and activation of circulating cells (leukocytes and platelets). As a consequence of the microcirculatory modifications, organ perfusion and oxygen delivery is impaired and high lactate levels can be produced by anaerobic glycolysis. Progressive hypoxemia[94] and lactate acidosis[95] limits ventricular oxygen consumption and contractility.

1.4.3 Myocardial injury in SIRS

Myocardial injury, detected by increase of cardiac troponins, is observed in setting of SIRS and sepsis in humans[96] and dogs[97, 98]. Troponins are regulatory proteins of the contractile apparatus of striated muscle cells (skeletal and cardiac myocytes). Each troponin protein has specific functions in contractile mechanism. Cardiac Troponin (cTn) is present only in cardiac muscle and Cardiac Troponin I (cTnI) is much more specific for detection of any damage to cardiac myocytes[99]. During myocardial injury, loss of membrane integrity, causes release of cTnI into the circulation, elevated cTnI levels indicate myocardial damage[100]. In dogs, cTnI is detectable within 4 to 6 hours and peaked between 10 to 16 h after cardiac injury[101]. Langhor et al in 2013 showed the clinical importance of cTnI as a marker of myocardial cell injury occurring in dogs with systemic inflammation and without primary cardiac disease. The study included 42 dogs presented with a diagnosis of trauma, neoplasia, gastrointestinal, respiratory, neurological and ematological diseases. Authors assessed systemic inflammation by measurement of CRP and several cytokines serum activity, they also evaluated myocardial cell damage by measuring cTnI concentration[97]. cTnI serum levels were higher in disease dogs than in control group and cTnI was found to be predictive of death in critically ill dogs with systemic inflammation[97, 98]. Myocardial injury associated with systemic inflammation has also been described in dogs with snake envenomation[102], ehrlichiosis[103], gastric dilation-vulvulus[104], babesiosis[105], pyometra[106], parvovirosis[107]and leishmaniasis[108].

Hagman et al reported that cTnI levels did not differ significantly in a pyometra patient group when compared with healthy dogs the same study showed that presence of SIRS was not associated with increased cTnI values[109].

1.4.4 Myocardial dysfunction in SIRS

Several veterinarian studies reveal that myocardial dysfunction accompanies sepsis and SIRS also in dogs. Bulter et al in 2008 demonstrated that cardiac output (CO), assessed by the Lithium Dilution Cardiac Output (LiDCO) method, oxygen delivery (DO), and cardiac index (CI) were significantly lower in a group of 18 dogs that meet SIRS criteria compared to healthy controls[111]. DO is the amount of oxygen delivered to the tissue and is calculated as the product of CO and arterial oxygen content, CI is the product of heart rate and stroke volume indexed to body surface area. LiDCO technique allows CO to be measured using only a peripheral or central venous catheter and a peripheral arterial catheter. The LiDCO method has been validated for use in dogs[110]. Since the heart rate did not differ between SIRS and control group, the authors hypothesized that the main cause of decreased in CO and CI, in the SIRS dogs, must be decreased stroke volume by reduced cardiac contractility secondary to inflammatory cytokines. CI, CO and OD were not significantly different between survivors and non-survivors[111]. Kenney and colleagues[64] reported a large-scale study of the association between outcome and organ system dysfunction in dogs with sepsis secondary to gastrointestinal tract leakage. Cardiovascular dysfunction was defined as hypotension sufficiently severe to require vasopressor treatment after surgery. Twenty (17.5%) of the 114 dogs met the criteria for cardiovascular dysfunction and only 2 of the 20 (10%) survived to discharge from the hospital. Echocardiography has been used in only a relatively small number of studies to assess cardiac function in dogs with SIRS[107, 112]. The most commonly used echocardiographic indices to assess global systolic function are the Fractional Shortening (FS%) and the Ejection Fraction (EF%). The FS% is obtained using the M-Mode scan of the left ventricle to measure the internal systolic and diastolic diameters. FS is calculated as follows:

$$FS\% = (LVIDd - LVIDs / LVIDd) \times 100$$

Were LVIDd is the Left Ventricular Internal Diameter in diastole and LVIDs is the Left Ventricular Internal Diameter in systole. FS% has several limitations, first, it measures only the radial contractility without considering the longitudinal and torsional motion of the left ventricle, second, it is highly dependent by preload and afterload conditions. A low FS% may be due to decreased radial contractility as well as increased afterload (vasoconstriction, systemic hypertension) or decreased preload (hypovolemia, dehydration). Conversely high FS% may be secondary to increased preload or decreased afterload. According to the Frank Starling principle, preload affect FS% because an increase in left ventricular diastolic size stretches the myofibers and increases their ability to shorten during systolic contraction. Moreover, FS% is negatively correlated to the heart rate, it decreases when the ventricle has less time to fill[113]. Normal FS% value in dogs is 34,4 ± 6,5[114]. FS < 25% is considered index of systolic dysfunction[115], although in some breeds, healthy subjects, can have a lower FS%[116].

Ejection Fraction (EF%) is an index of global systolic function derived from ventricular volumes. It is calculated as follows:

$$EF\% = (LV\ DV - LV\ SV / LV\ DV) \times 100$$

Where LV DV is the Left Ventricular Diastolic Volume and LV SV is the Left Ventricular Systolic Volume.

EF < 40% is considered index of systolic dysfunction[115].

LV volumes can be estimated by M-Mode and by Bi-Dimensional echocardiography. M-Mode derived LV volumes are calculated by the Teicholz equation as follows:

$$LV\ DV = (7 \times (LVIDd)^3) / (2,4 + LVIDd)$$

and

$$LV\ SV = (7 \times (LVIDs)^3) / (2,4 + LVIDs)$$

Were LV DV is the Left Ventricular Diastolic Volume, LV SV is the Left Ventricular Systolic Volume, LVIDd is the Left Ventricular Diameter in diastole, LVIDs is the Left Ventricular Diameter in systolie.

The Teicholz formula is a geometric method based upon the assumption that the LV chamber is an ellipse. Teicholz equation overestimates the LV volume in dogs, especially in the case of volume overload[117], this is because the geometric method does not use the LV length but only the transversal diameter.

Two-Dimensional derived LV volumes are achieved by the Simpson method. The ventricular volumes are derived from the left ventricular diastolic and systolic area, obtained by drawing the endocardial contour of the LV on a 2D image (right parasternal long axis or left apical 4 or 2 chambers views). Simpson's derived method shows the best correlation with real volumes in the diseased heart[117].

Another commonly used index of systolic function is the End Systolic Volume Index (ESVI). It represents the LV systolic volume indexed to the body surface area (BSA). The normal values depend on the method used to calculate volume.

Spectral Doppler may also be used to obtain left ventricular systolic indices. The LV Pre Ejection Period (PEP) is the time interval between the beginning of the Q wave on the simultaneous ECG and the beginning of the ventricular ejection on the spectral Doppler trace. LV Ejection Time (ET) is the time interval between the beginning and the end of the aortic wave on the spectral Doppler. A systolic dysfunction leads to an increase of the PEP, as a consequence there is an increase in the PEP/ET ratio[118].

In 2006, Nelson and Thompson[119] reported a retrospective study of 16 dogs with left ventricular dysfunction associated to critical illnesses. Critical illness was defined as metabolic derangements that required intensive care to sustain life, and left ventricular systolic dysfunction was defined as a FS < 26% and/or an EF < 46%. Dogs with a LV PEP/ET > 0.4 were also considered to have systolic dysfunction. Mitral valve inflow E/A ratio < 1 were interpreted as ventricular diastolic dysfunction. Dogs that had an obvious endocarditis and breeds of dogs

with an increased incidence of dilated cardiomyopathy were excluded from the study because of their greater risk of cardiac dysfunction. All the dogs were normally hydrated at the time of echocardiographic exam. The two most common diseases identified producing critical illness with left ventricular systolic dysfunction were sepsis (n 5) and cancer (n 5), within the cancer group 3 dogs had lymphosarcoma, 1 mesothelioma and 1 pulmonary adenocarcinoma. Other diseases diagnosed in affected dogs were pancreatitis, intestinal bowel disease (IBD), immune-mediated haemolytic anaemia, immune polyartropathy and coccidiomycosis. Twelve of the 16 dogs (75%) died or were euthanized within 15 days of hospital admission, with an average time until death of 3.6 days. Ten dogs had necropsy examination, which did not reveal gross or histological evidence of cardiac disease in any dog. Treatment regimens for the dogs varied considerably so comparison between survivors and non-survivors was not performed. The 4 dogs that were discharged had follow-up of 20 days, 3.5 months, 4 months, and 2 years respectively. Longitudinal echocardiographic data were available only for a dog with immune-mediated polyarthropathy, anaemia, and hyperglobulinemia that was still alive 2 years after hospitalization. The FS had risen from 21% at the time of hospitalization to 34% 2 years later, suggesting reversible myocardial depression[119].

Dickinson et al[120] reported a case of a 5-months-old 22 Kg female Rhodesian Ridgeback with reversible myocardial depression associated with septic arthritis. At the time of admission the dog fulfilled the SIRS criteria (tachypnea, fever and band neutrophils). Systolic dysfunction was assessed with an echocardiographic exam, which showed a dilated, hypokinetic left ventricle and a decrease in FS%. Right ventricle was also dilated. The Left Ventricular Systolic Diameter (LVIDs), the End Systolic Volume Index (ESVI) and the E-Point to Septal Separation (EPSS) were all increased. The dog recovered well, and, three months later an echocardiographic examination showed good left ventricular contractile function and normal cardiac dimensions. All evidence of previously noted myocardial dysfunction had resolved.

Recently Kocaturk et al[121] demonstrated myocardial injury and myocardial depression in dogs with SIRS induced by Canine Parvovirus (CPV). EF%, FS% and the Tei index were used to assess left ventricular systolic and diastolic dysfunction. cTnI levels were used to determine myocardial injury. Tei index calculated for non-survival dogs were significantly higher than that of survival and control dogs. Lower FS% and EF% were observed in non-survival dogs, compared with survival and control dogs. There were no significant differences in EF% and FS% between healthy and SIRS survivors dogs. The Tei index, also called Index of Myocardial Performance (IMP) is a Doppler derived index of global myocardial systolic and diastolic function developed by Tei[122].

In the 22nd ECVIM-CA congress, Gommeren[112] et al presented an oral research communication about echocardiographic evaluation of cardiac dimensions and left ventricular systolic function in 37 dogs with SIRS (infection n=6, neoplasia n=4, trauma=4, gastric dilation-volvulus n=4, other gastro-intestinal disease n=4 and miscellaneous diseases n=15) and without primary cardiac disease. Left ventricular systolic function was assessed through FS% and EF%. In this study 28 patients (76%) survived. The authors concluded that in this population of SIRS patients, no echocardiographic evidence of cardiac dysfunction was demonstrated[112].

The results of these studies suggest that myocardial injury and myocardial dysfunction are common findings in dogs suffering from SIRS of infectious or non-infectious origin. However, the commonly used echocardiographic indices of systolic function, such as FS% and EF%, have not been always sensitive enough to detect systolic dysfunction in dogs suffering from SIRS[112]. In fact, echocardiographic evidence of systolic impairment has been demonstrated mostly in SIRS dogs that did not survive compared to survivors[119, 121]. FS% and EF% were reduced only in case of severe cardiovascular impairment as seen in multiple organ dysfunction or failure[123]. Several studies in humans and in a porcine model of sepsis[124] have shown evidence of left ventricular systolic dysfunction with preserved Ejection Fraction in patients with sepsis[125, 126] and

other conditions of heart failure[127]. During SIRS mild to moderate systolic dysfunction may not be revealed by the decrease of FS% or EF% due to the reduction in preload and afterload and the increase in heart rate (HR).

1.5 Advanced techniques in Veterinary Echocardiography

New cardiovascular ultrasound imaging techniques have been developed over the last 15 years. They include Tissue Doppler Imaging (TDI) and Speckle Tracking Echocardiography (STE). These techniques allow analysing myocardial displacement, velocity and deformation that occur during the cardiac cycle. The active systolic movements of the left ventricle are complex and have three major components:

1) **Longitudinal** motion with the base moving toward the apex;
2) **Radial** motion, during which the left ventricular posterior wall (LVPW) and the interventricular septum (IVS) converge toward a geometric centre located in the centre of the left ventricular chamber. The radial motion is associated with a circumferential deformation and radial thickening of the myocardium;
3) **Torsional** motion of the left ventricle, it is due to the opposite rotational movements of the base and apex in relation to an imaginary long axis line from apex to base. When the heart is viewed from the apex, the base rotate in clockwise direction and the apex rotate in counter clockwise direction[128].

The complexity of ventricular kinetic is related to the geometrical layout of the myocardial fibres. They are set in three layers: sub-endocardial, mid-wall and sub-epicardial. Fibre orientation changes gradually from a right handed helix layout in the sub-endocardial layer to a circular layout in the midwall layer, and then to a left-handed helix layout in the sub-epicardial layer[113]. Radially oriented fibres of the middle layer are predominant at the base compared to the apex wall of the left ventricle.

There are also passive movements of the LV like the translation movements, corresponding to the displacement of the heart as a whole within the thoracic

cavity and the dragging movements by which a myocardial segment is dragged by the contraction of an adjacent segment (e.g. scar tissue which is unable to contract is dragged by adjacent vital myocardium during systole).

Tissue Doppler and Speckle Tracking Imaging have introduced new echocardiographic indices of myocardial function as myocardial displacement, velocity of displacement, deformation (Strain) and velocity of deformation (Strain Rate).

TDI is a Doppler technique that enables to quantify global and regional myocardial function, measuring the radial and longitudinal myocardial velocities throughout the entire cardiac cycle. From the myocardial velocity (expressed in cm/sec), Tissue Tracking Imaging (a technique derived from TDI) allows to calculate the myocardial displacement (expressed in mm) and the deformation parameters as Strain (St) and Strain Rate (StR). TDI has been the first echocardiographic method from which myocardial deformation parameters could be derived. However, TDI, has several limitations, in fact, being a Doppler technique it is angle dependent, and myocardial velocities assessed by TDI do not discriminate between actively contracting myocardium and passive motion due to translational movement and tethering effect[129]. The derived parameters of deformation, St and StR, partially reduce these limitations.

Strain (St) is the percentage of deformation of the myocardium during the cardiac cycle (Figure 3). It is calculated with the following formula:

$$St = L - L_0 / L_0$$

Where L is the length of the myocardial segment after deformation, and L_0 is the basal length of the segment. By convention, depending on the direction, a lengthening or thickening deformation is given a positive value, whereas a shortening or thinning deformation is given a negative one. Strain is expressed in per cent (%).

Strain Rate (StR) is defined as the velocity at which deformation occurs (Figure 4). It is equal to the Strain divided by Δt:

$$StR = St/\Delta t$$

It is expressed in s^{-1}; in other words, if the same Strain value is reached in half the time, the Strain Rate value will be doubled.

Speckle-Tracking Echocardiography (STE) is a new non-invasive ultrasound imaging technique that allows an objective and quantitative evaluation of global and regional myocardial function using a completely different algorithm compared to TDI-derived methods to calculate deformation. Speckles are groups of myocardial pixels that are created by the interaction (reflexion, scattering and interferences) of ultrasonic beams and the myocardium during the 2-dimensional exam. Single speckles are merged in functional units (kernels) that are in turn univocally identifiable given the peculiar disposition of the speckles. They represent the natural acoustic markers of the myocardial tissue; each kernel constitutes a sort of ultrasound fingerprint that can be tracked by the software from frame to frame during the entire cardiac cycle[128, 130].

STE allows distinguishing between active and passive movements of myocardium. STE derived Strain is directly calculated from the frame-to-frame motion of speckle patterns and not from myocardial velocities (Figure 1 and 2). Through analysis of the motion of each kernel that composes a routine 2-dimensional grey scale image, the system, without using the Doppler signal, can measure global and regional displacement, velocity of displacement, Strain and Strain Rate, in longitudinal, radial and circumferential directions[130] (Figure 2). It can also quantify rotational movements such as rotation, twist and torsion of the myocardium. The protocols for acquisition are not much different from routine echocardiograms. The endocardial border needs to be well delineated and well visualized for reliable tracking, and for that, images acquired should be of high quality. The optimal frame rate should be 60 – 110 frames per second (FPS). It is preferable to keep the sector width and depth minimal to focus on the structure of interest. As the values are averaged for the final results, using the software during final processing, three consecutive cardiac cycles are obtained. Considering the close dependence of STE and single-cardiac-cycle Strain analysis, it is not possible to conduct a study in patients with non-sinusal rhythm. There are

different algorithms used by different vendors in tracking these kernels. The region of interest (ROI) has to be outlined manually even if vendors have incorporated tools to help users identify tracking reliability. The LV is evaluated by tracing the endocardial border by point and click method. The epicardium is automatically traced by the system, but the wall thickness can be manually adjusted.

To obtain the complete STE analysis of the global LV longitudinal and radial function from the long axis views the operator needs to analyse three left apical views: left apical two, three and four chambers (Figure 5). The ways myocardial segments are divided widely vary among the vendors, but in general, a 16 to 18-segment LV model is used. Segments for which no adequate image quality can be obtained are rejected by the software and excluded from the analysis. Once the region of interest is optimized, the software generates Strain curves for each selected myocardial segment (Figure 6). From these curves, the operator can obtain regional and global peak and time-to-peak values. Global values of LV deformation parameters are obtained by averaging values observed in all segments. By the Automated Function Imaging (AFI) system, which allows a semiautomatic analysis of STE parameters, the results of each view are merged and represented in the bull's-eye view of segmental parameters of deformation (Figure 7). Each analysed segment corresponds to a different coronary territory.

Parasternal short-axis views one from the basal short-axis view, obtained at the tips of the mitral valve leaflets and the other at the apex, proximal to the end of LV cavity, are necessary to analyse radial, circumferential and torsional deformation of the left ventricular myocardium (Figure 5).

Longitudinal Strain (LS) represents the myocardial deformation directed from the base to the apex (Figure 2). During systole, ventricular myocardial fibres shorten with a translational movement from the base to the apex; the consequent reduction of the distance between single kernels is represented by negative St curves (Figure 6). During diastole the distance between kernels increase therefore the St value is positive. The Left Ventricular Global Longitudinal Strain (LV

GLS) has been recently validated as a quantitative index of global LV function in humans[131]. Culwell et al in 2011 found a significant linear correlation between 2D-STE derived LV GLS and load-independent indices of systolic function obtained through the thermodiluition technique in dogs[132]. Similarly, Amudsen et al, in 2006, identified a strong positive correlation between 2D-STE derived LV GLS and LV long-axis St obtained from Tagged MRI *(r = 0,87; p< 0,001)* in humans as well as between 2D-STE derived LV GLS and LV longitudinal St measured by sonomicrometry *(r = 0,9; p< 0,001)* in dogs[133]. MRI tagging is currently considered the non-invasive gold standard for evaluation of systolic deformation[134]. The results of these studies suggest that the LV GLS can be considered as a non-invasive, load-independent index of LV systolic function and therefore of LV contractility.

Radial Strain represents radially directed myocardial deformation, toward the centre of the LV cavity. It indicates the LV thickening (systole) and thinning (diastole) deformation during the cardiac cycle; consequently the radial St values during systole are represented by positive curves. Radial St measurements can be obtained by STE analysis of both LV short-axis and long axis views.

Circumferential Strain represents LV myocardial fibre shortening along the circular perimeter observed on a short-axis view. Consequently, during systole, for circumferential speckle-to-speckle distance reduction, circumferential strain measurements are represented by negative curves.

Parasternal short-axis views, one from the basal short-axis view obtained at the tips of the mitral leaflets, the other at the apex, barely proximal to the end of LV cavity, are necessary for rotation, twist, and torsion analysis.

Rotation is the measure of the rotational movement of the myocardium in relation to an imaginary long axis line from the apex to the base drawn through the middle of LV cavity. Clockwise rotations are assigned a negative value (e.g. -10°) and counter clockwise rotations a positive value (e.g. +10°).

Twist or torsion measures the algebraic difference in rotation between the apex and the base. For example, if the apex moves 30 ° counter clockwise and the base

moves 15 ° clockwise, then the twist will be 45 ° (30 - (- 15) = 30 + 15 = 45°. The rate and total duration of twist can also be measured.

Untwisting: Growing attention has been also recently given to the role of untwisting in diastolic LV filling mechanics. Untwisting velocity is thought to be a critical initial manifestation of active relaxation, which makes this measurement relevant for investigating diastole and, mainly, isovolumic relaxation because it seems to be less dependent on load compared to other diastolic parameters.

All the 2D-STE measurements can be individualized for each of the myocardial segment or can be expressed as global values when all the segmental values are averaged. St and StR can be measured not only for the LV but also for the Right Ventricle (RV) and Left and Right Atria[135] (LA and RA), but these are much less commonly used in the clinical setting and some have not been fully validated.

In canine cardiology 2D-STE have been used to measure LV Radial St[136], LV Torsion[137], Longitudinal St and StR[138] for both endomyocardial (ENDO) and epimyocardial (EPI) layers[139]. In all the studies the 2D-STE has been shown to have a good repeatability and reproducibility. Moreover, 2D-STE has been validated in dogs against sonomicrometry, tagged MRI[133], Tissue Doppler Imaging[136, 138] and thermodilution technique[132]. Suzuky et al demonstrated that age[140] and heart rate[141] did not exert a significant influence on 2D-STE derived longitudinal systolic St and StR in healthy dogs.

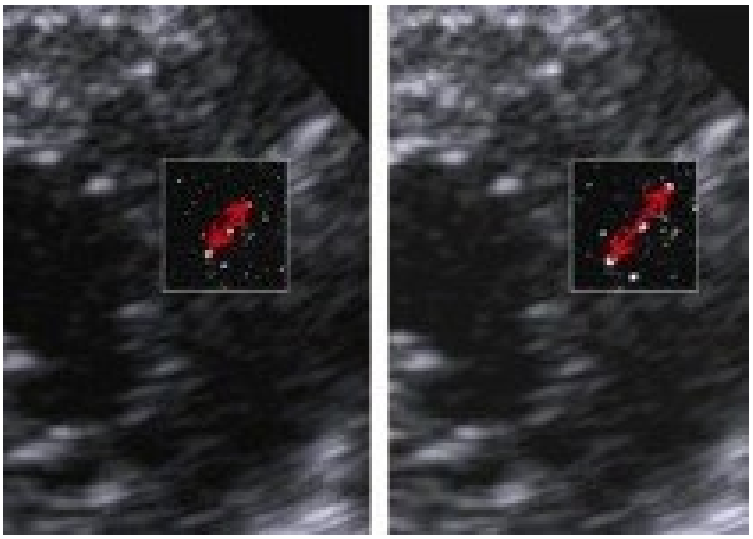

Figure 1. Change in distance between kernels during cardiac cycle

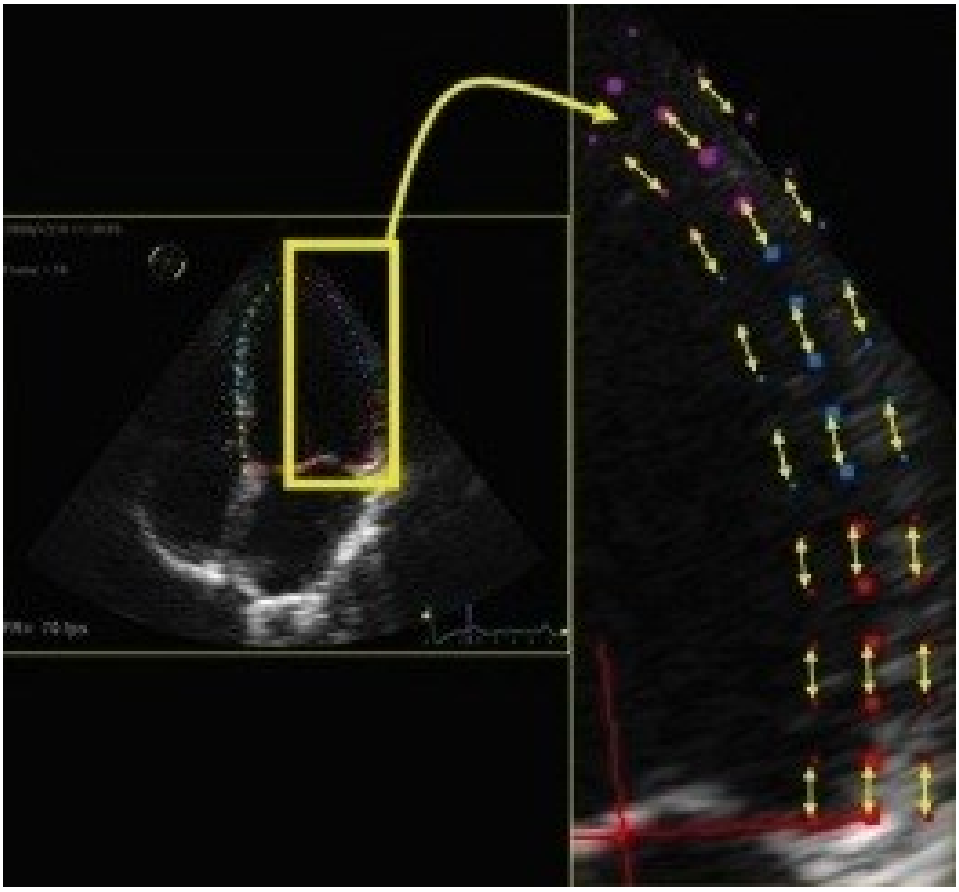

Figure 2. Longitudinal motion of kernels during cardiac cycle

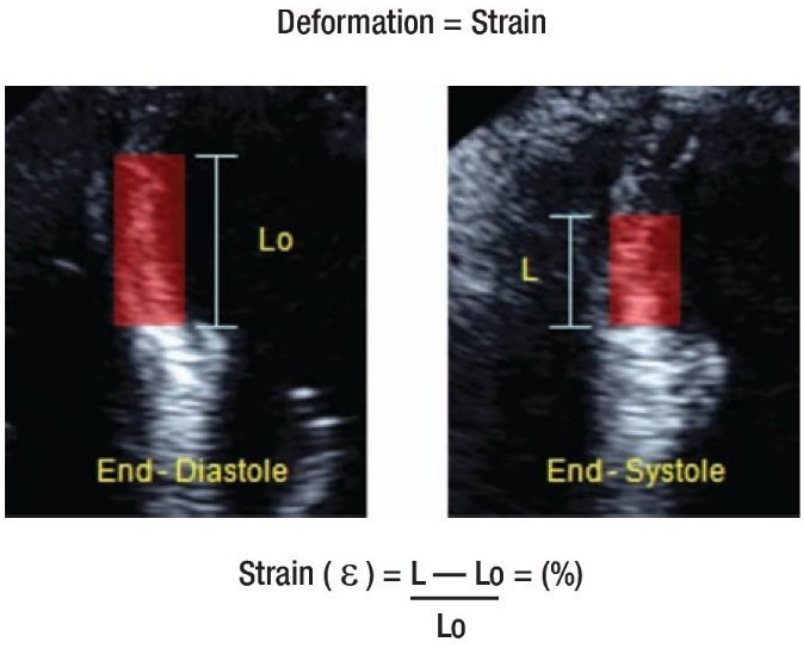

Figure 3. Longitudinal Strain of the Left Ventricle

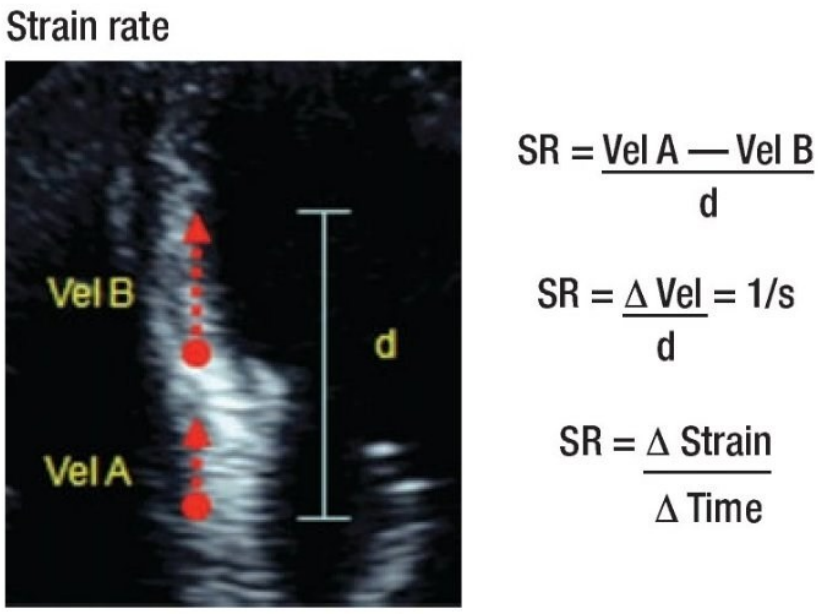

Figure 4. Longitudinal Strain Rate of the Left Ventricle

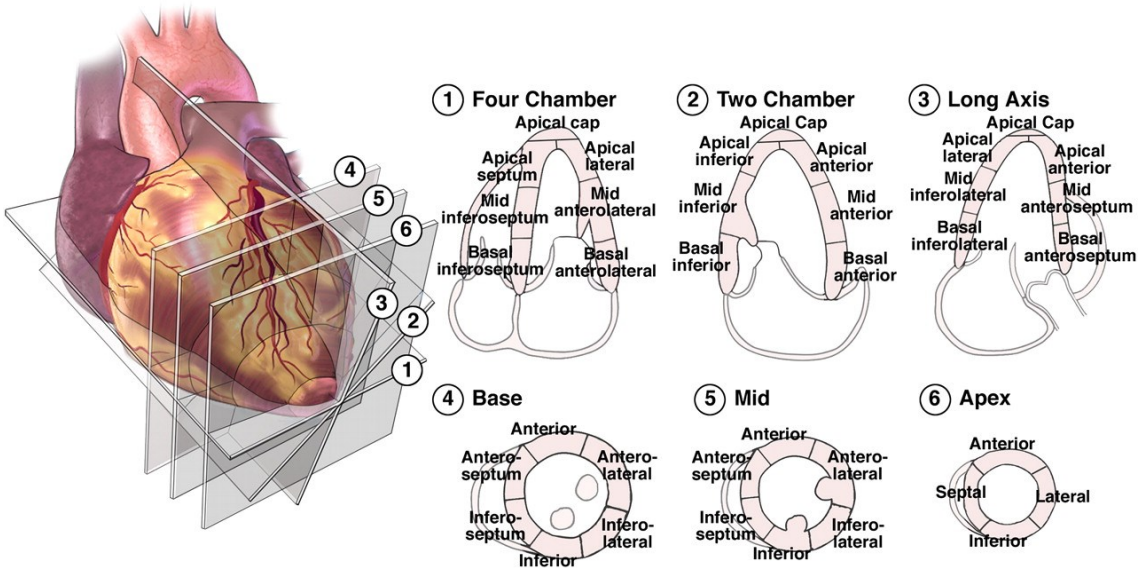

Figure 5. Apical and transversal view commonly used to evaluate the longitudinal, radial an torsional deformations of the LV

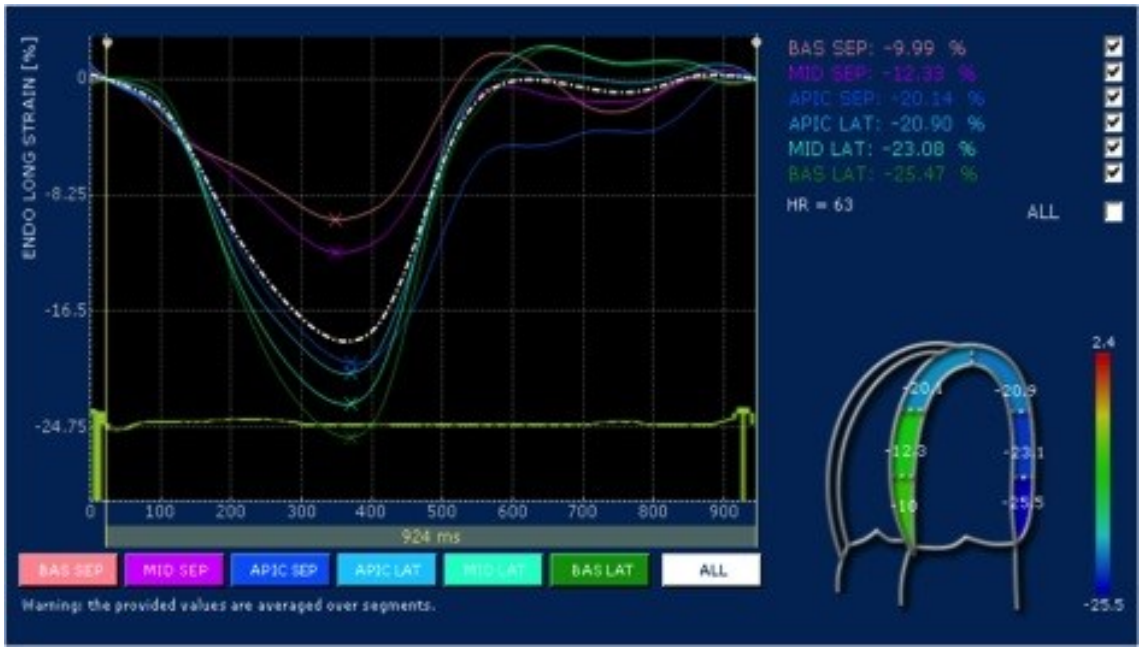

Figure 6. Graphic representation of longitudinal segmental Strain of the LV

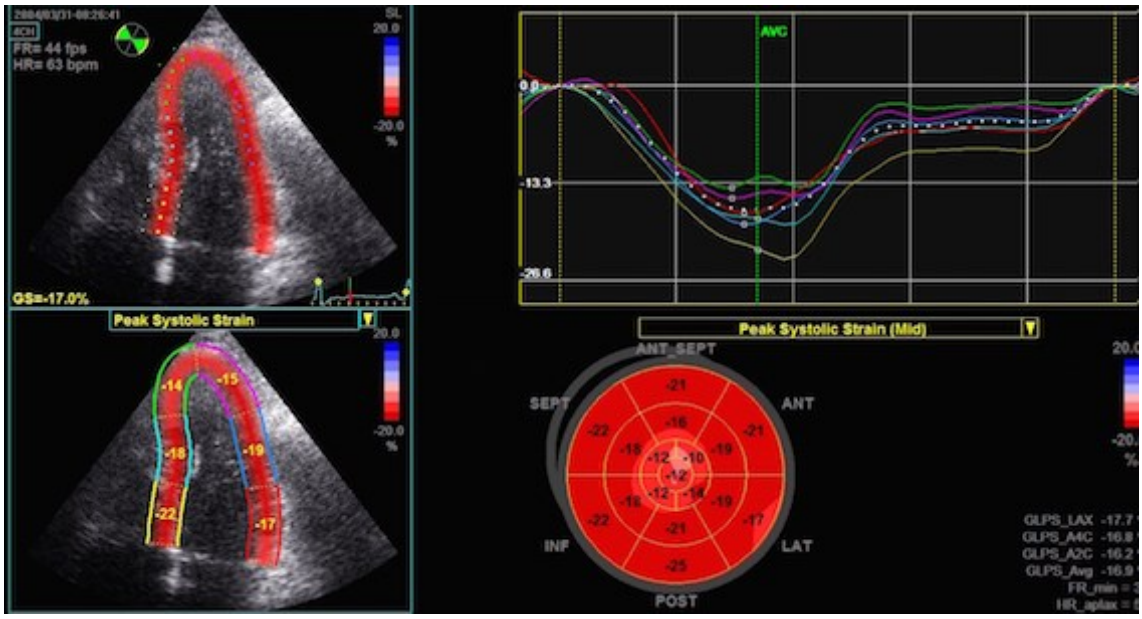

Figure 7. Graphic representation of longitudinal segmental Strain of the LV, the Bull's eye

2. OBJECTIVE OF THE STUDY

Global systolic function is influenced by several factors including preload, afterload, contractility, distensibility, coordinate contraction and heart rate. Assessment of global left ventricular systolic function is of paramount importance in dogs suffering from SIRS because it could influence the prognosis and the treatment decision. There is evidence that endotoxin[77] and several other molecules[16] contribute to the activation of an endogenous cascade of local and systemic inflammatory mediators, such as interleukins[83], which reduces myocardial contractility in humans and animals suffering from SIRS and sepsis[82]. It is also known that dogs with SIRS of infectious or non-infectious origin have high levels of interleukins in their bloodstream[14, 19, 20]. Previous studies conducted in dogs suffering from SIRS suggest that the conventional echocardiographic indices, such as LV Fractional Shortening (FS%) and Ejection Fraction (EF%), are able to detect systolic dysfunction only in severe SIRS or in the late stage of the disease in fact, low FS% and EF%, were found especially in non-survival dogs suffering from SIRS and sepsis[107, 119]. EF% and FS% as well as systolic time intervals are not sensitive enough to detect mild to moderate or early systolic dysfunction in dogs because they are highly dependent on loading conditions and heart rate[132]. Tagged MRI is considered to be the absolute non-invasive gold standard for measurement of LV contractile function[134], but it is expensive and requires anaesthesia, which depresses contractility and may be a risk for critically ill patients. Several studies, including people and other animal models with sepsis, have revealed the ability of the 2D-STE deformation parameters in detecting LV systolic dysfunction before the reduction in the LV EF% could be seen[124, 126]. The aim of the present study was to evaluate the systolic function in dogs with SIRS using 2D-Speckle Tracking Echocardiography (2D-STE). We tested the hypothesis that 2D-STE may detect LV systolic dysfunction not diagnosed by conventional echocardiography in dogs with Systemic Inflammatory Response Syndrome of both infectious and non-infectious origin. A second objective of the study was to compare serum

Cardiac Troponin I (cTnI) levels among dogs with SIRS and healthy dogs as well as to evaluate if there were correlation between systolic function, serum cTnI and C-reactive Protein (CRP) in dogs suffering from SIRS.

3. MATERIALS AND METHODS

Data were collected during 2014 at the Small Animal Hospital, University of Sassari. Permission for the participation of each dog was obtained from the owner.

3.1 Case selection

3.1.1 SIRS group

Dogs presented to the Critical Care Service of the Small Animal Hospital, with SIRS, secondary to various pathologies, were prospectively included in this observational clinical study. SIRS was diagnosed when a dog fulfilled at least two of the established SIRS criteria as described in a previous publication [3]:

1. Hypo-or-hyperthermia (≤ 37,8° C or ≥ 39,7° C)
2. Tachycardia (≥160 beats per minute)
3. Tachypnea (≥ 40 breaths/min)
4. PCO_2 (≤ 32 mm/Hg)
5. A WBC count ≥ 12000 WBCs/µl (leucocytosis) or ≤ 4000 WBCs/µl (leukopenia) or ≥ 10% immature (band) neutrophils.

To increase specificity of SIRS criteria we excluded from the study group dogs with CRP values lower than 1,07 mg/dl[142].

The exclusion criteria for the study group were:

- Giant breeds or breed predisposed to dilated cardiomyopathy (DCM), in particular Doberman Pinscher, Newfoundland, Portuguese Water dog, Boxer, Great Dane, Cocker Spaniel, Saint Bernard and Irish Wolfhound;
- Dogs less than 1 year of age;
- Previous diagnosis of myocardial disease;
- Echocardiographic evidence of congenital cardiac disease;
- Moderate or severe mitral regurgitation (Regurgitant Jet Area/ Left Atrium Area ≥ 30%)[143, 144] with or without symptoms;
- Echocardiographic evidence of cardiac remodelling (stage B_2 or more)[145];

- Echocardiographic evidence of moderate to severe pulmonary hypertension [146, 147];
- Have received anaesthetic, sedative or opioid treatment during the previous 12 hours;
- Have received corticosteroids or non-steroidal anti-inflammatory drugs during the previous 12 hours;
- Have been treated with a know cardio toxic drug (e.g. Doxorubicin);
- Presence of persistent arrhythmias identified during the echocardiographic exam;
- Clinical evidence or previous diagnosis of pregnancy;

3.1.2 Control group

The control group consisted of healthy dogs recruited from the veterinary community as a control population of this study. Dogs of the control group were considered healthy based on physical examination, cell blood count (CBC), biochemical profile, serum protein electrophoresis, indirect blood pressure measurement, echocardiographic exam (with simultaneous ECG) and serum levels of CRP and cTn-I.

The exclusion criteria for the control group were:

- Giant breeds or breed predisposed to dilated cardiomyopathy (DCM), in particular Doberman Pinscher, Newfoundland, Portuguese Water dog, Boxer, Great Dane, Cocker Spaniel, Saint Bernard and Irish Wolfhound;
- Previous diagnosis of myocardial disease;
- Echocardiographic evidence of congenital cardiac disease;
- Moderate or severe mitral regurgitation (Regurgitant Jet Area/ Left Atrium Area $\geq$ 30%)[143, 144] with or without symptoms;
- Echocardiographic evidence of cardiac remodelling (stage B_2 or more)[145];
- Echocardiographic evidence of moderate to severe pulmonary hypertension [146, 147];

- Have received anaesthetic, sedative or opioid treatment during the previous 12 hours;
- Have been treated with a known cardio toxic drug (e.g. Doxorubicin);
- Presence of persistent arrhythmias identified during the echocardiographic exam;
- Clinical evidence or previous diagnosis of pregnancy;
- Serum CRP levels ≥ 1,07 mg/dl;

3.2 Data collection

At the time of admission, after have recorded the patient's medical history, each dog, from both groups SIRS and control, was submitted to:

- Complete physical examination;
- Blood collection;
- Indirect blood pressure (BP) measurement using a high definition oscillometric blood pressure monitor (Memodiagnostic MD 15/90 Pro, S+B medVET, Germany). BP was considered normal when values were included within the following range: systolic 131 ± 20 mm/Hg, diastolic 74 ± 15 mm/Hg and mean 97 ± 16 mm/Hg as reported by Bodey et al[148];
- Echocardiographic examination with simultaneous ECG;
- Additional diagnostic procedures (e.g., radiography, ultrasonography, endoscopy, exploratory laparotomy, cytology, and histopathology) for individual dogs were performed, depending on the medical condition, to achieve the correct diagnosis.

3.2.1 Blood collection

8.0 ml of blood were collected from the jugular vein. Immediately 1.0 ml of the blood was mixed with the anticoagulant (K3-EDTA) for CBC analysis. The rest of the blood was put into a sterile tube, allowed to clot for two hours at room temperature (20-22°) then centrifuged (1000g) for 15 minutes and the serum was collected aseptically. Grossly haemolysed samples were excluded. Lipemic samples were ultracentrifuged to separate the sample into lipemic and non-

lipemic layers, and the latter were used for analysis. 2 ml of serum were stored at -80°C for a maximum of 2 months, until analysis for CRP and cTn-I.

A clinical biochemistry profile and a CBC were performed using, respectively, an automated haematology analyser (Lasercyte, Idexx Laboratories, Westbrook, ME, USA) and a clinical chemistry analyser (ABX Pentra 400, Horiba Medical, Japan) on the day of collection.

Serum CRP concentrations were measured by an immunoturbidimetric assay for canine CRP (catalogue number CP2572, Randox Laboratories Limited, Crumlin, County Antrim, UK) on a clinical chemistry analyser (ABX Pentra 400, Horiba Medical, Japan), according to the manufacturer's instructions. The reference range of the serum CRP concentration was considered from 0 to 1,07 mg/dl based on the manufacturer's data sheet and previous report[142].

Serum cTn-I were measured using a quantitative sandwich enzyme immunoassay technique for detection of canine cTn-I (Canine cardiac Troponin I ELISA Kit, Immunological Science, Rome) on an absorbance microplate reader, Infinite F50, Tecan, Switzerland, according to the manufacturer's instructions. The reference range of the serum cTn-I concentration was considered from 0,03 to 0,07 ng/ml based on a previous report[149].

3.2.2 Echocardiographic examination

Each echocardiographic exam was performed by a single experienced operator (AC) with a portable ultrasound unit (*My Lab Alpha*, Esaote, Italy) equipped with a multi frequency 2-5 MHz phased array transducer. The dogs were positioned alternately in right and left lateral recumbence on a raised table with a central opening, designed for veterinary echocardiographic examination. The dogs were examined by two-dimensional, M-mode, Doppler and 2-D Speckle Tracking echocardiography with simultaneous lead II ECG. All images and loops were stored and analysed off-line with the same ultrasonographic unit. Each exam was analysed by the same observer (AC). Each measurement was repeated 3 times, and mean values were calculated for further statistical analysis.

M-mode and 2D echocardiographic cine loops and images were performed and measured as recommended in the Guidelines of the American Association of Echocardiography[150]. M-mode echocardiography of the LV was obtained from the right parasternal short axis view. The LV-diameter was measured in end diastole (LVIDd) and end systole (LVIDs). End diastole was defined as the beginning of the QRS complex and end systole as the maximal approximation of septum and LV posterior wall[151]. Measurements of 3 consecutive cardiac cycles were used to calculate the mean values. The linear measurements of LV were normalized using body weight according to the results of a regression analysis reported by Cornell et al[152].

Endocardial Fractional Shortening (FS %) was calculated as follows:

$$FS\ (\%) = (LVIDd - LVIDs / LVIDd) \times 100$$

Where LVIDd is the Left Ventricle Internal Diameter in diastole and LVIDs is the Left Ventricle Internal Diameter in systole.

FS < 25% was considered index of systolic dysfunction[115].

M-mode echocardiography was also used to calculate LV volumes by use of the Teicholz equation[153]. LV volumes were also calculated from 2D loops using the monoplane Simpson Method of Disks (SMOD). It was performed in right parasternal long-axis view as described by Wess et al[154]. End diastole was defined as the beginning of the QRS complex at the time of mitral valve closure, and end systole was defined as the minimal cavity area before mitral valve opening. The SMOD measurement required manual tracing along the endocardial border in the selected end-systolic and end-diastolic images from one side of the mitral annulus to the other, whereas papillary muscles and trabeculae were included in the LV volume calculation. The maximal length of the LV cavity was measured from the middle of the mitral annulus to the endocardial border of the LV apex. The software of the ultrasound unit automatically calculated the LV systolic and diastolic volumes by use of the summation of the 15 elliptical disks.

We calculated EF% using LV volumes obtained from both methods (Teicholz and Simpson) using the following formula:

$$EF\ (\%) = (LV\ EDV - LV\ ESV\ /\ LV\ EDV)\ x\ 100$$

Where LV EDV is the Left Ventricle End Diastolic Volume and LV ESV is the Left Ventricle End Systolic Volume.

EF < 40% was considered index of systolic dysfunction[115].

We assessed the global left ventricular systolic function also evaluating the Doppler-derived systolic time intervals, Left Ventricular Pre-Ejection Period (LV-PEP) and Left Ventricular Ejection Time (LV-ET)[118,155]. Using a left apical view, with the dog in left lateral recumbence, we obtained the Pulsed Wave (PW) spectral Doppler aortic flow profile. Ejection Time (ET) was measured from the onset to the end of the aortic flow profile; Pre-Ejection Period (PEP) was measured from the onset of the electrocardiographic QRS complex to the onset of the aortic flow wave on the spectral trace. The LVPEP/LVET ratio was calculated in each instance and a value greater than 0,4 was considered an index of systolic dysfunction[115,119].

3.2.3 Two-dimensional Speckle Tracking Echocardiography

Two-dimensional digital cine loops, with duration of one cardiac cycle each, were acquired using a FR between 50 and 70 frame per second and with a high quality simultaneous ECG from the following left apical views:, and

- Left apical 4 chambers view (4Ch) showing both atria and ventricles;
- Left apical 2 chambers view (2Ch) showing LA and LV;
- Left apical 3 chambers view (3Ch) showing LA, LV and ascending aorta, also called apical long-axis image[156];

All cineloops were later analysed by the same observer (AC) using the software packages 2D-XStrain™ and XStrain-4D™ (Esaote, Florence, Italy). 2D-XStrain™ is a dedicated border tracking software which made a 2D-Speckle Tracking analysis of each apical view, while, XStrain 4D™ fused and processed the 2D Speckle tracking information, obtained from the three 2D left apical views, creating a LV model in a 3D space and giving global LV deformation parameters. An end-diastolic frame with optimal endocardial and epicardial border outlining was selected. Three starting points (1 on each mitral valve hinge

point and 1 at the apex) were manually set according to instructions provided by the software producer. The system used provides an assisted mode called Aided Heart Segmentation (Esaote, Florence, Italy) for the initial tracking points insertion. It assists the operator in inserting well equi-spaced tracking points over the 2D images. A total of 13 equidistant points for each border were tracked in each 2D apical view. From these points, the software automatically tracked the endocardial and epicardial border and divided the LV wall in 12 segments. If the automatically positioned points were not correctly disposed along the cardiac border they were manually adjusted. A visual inspection at decreased playback speed was performed. If one or more segments had poor tracking, due to echo drop out or artefacts, the cineloop from that view was discarded, because points belonging to one segment are shared between two segments, and could therefore have affected also results of good quality segments from the same view[139]. Only cardiac cycles with adequate tracking quality and with no signs of arrhythmia, aside from respiratory sinus arrhythmia, were included. The 2D-XStrain™ software then performed the tracking of each segment over time. The software automatically divided the myocardial wall into a basal, a mid-ventricular, and an apical myocardial region. Basal, mid and apical LV endocardial and epicardial longitudinal and transversal variables of myocardial deformation were obtained by averaging the corresponding values of all segments at each level. Graphics and curves of studied variables were automatically displayed and the peak systolic values of longitudinal and transversal Strain (St), Strain Rate (StR), displacement and velocity were shown for the endocardial (ENDO) and epicardial (EPI) regions of the myocardium (basal, mid and apical region). Mean LV ENDO and EPI longitudinal and transversal variables were obtained by averaging the corresponding values of all 6 regions for each view.

By fusing 2D-Speckle Tracking information obtained from apical 4Ch, 2Ch and 3Ch the XStrain-4D software created a LV model in a 3D space providing LV global and regional parameters of deformation and LV volumes. The heart rate (HR) should not have been different more than 10% in the 3 apical views.

The global 2D-STE values for each regional variable (LV basal, mid-level and apical) were calculated as the mean value of the segments in each view. Regional values were averaged to obtain LV global mean values of displacement (mm), velocity (mm/sec), Strain (%) and Strain Rate (1/sec) of the endocardial (ENDO) and the epicardial (EPI) border.

The following LV global and regional variables were obtained:

1) Peak transversal displacement of endocardial border (mm);
2) Peak transversal displacement of epicardial border (mm);
3) Peak longitudinal displacement of endocardial border (mm);
4) Peak longitudinal displacement of epicardial border (mm);
5) Peak transversal velocity of endocardial border (mm/sec);
6) Peak transversal velocity of epicardial border (mm/sec);
7) Peak longitudinal velocity of endocardial border (mm/sec);
8) Peak longitudinal velocity of epicardial border (mm/sec);
9) Peak longitudinal epicardial Strain Rate ;
10) Peak longitudinal endocardial Strain Rate;
11) Peak longitudinal epicardial Strain;
12) Peak longitudinal endocardial Strain;
13) Peak transversal Strain;
14) Peak transversal Strain rate;

From the LV apical views transversal or radial displacement and velocity were defined as the myocardial displacement and velocity of displacement in a direction perpendicular to the endocardial border. Both variables were assumed to be positive when directed towards the cavity (contraction)[157].

From the LV apical views longitudinal displacement and velocity were defined as the myocardial displacement and velocity of displacement in a direction tangential to the endocardial border. Both variables were assumed to be positive when directed from the base towards the apex (contraction)[157].

Peak systolic longitudinal and transversal displacement, velocity, Strain (St), Strain Rate (StR), were defined as the maximal deflection of the respective

curves during the ejection phase, defined from the ECG. Peak values of 2D-STE variables were measured from three cardiac cycles and then averaged.

A total of 57 STE variables were analysed, including the STE derived EF%, calculated from the LV volumes obtained with the XStrain-4D software.

3.3 Variability study

The intra-operator within-day and between-day variability for acquisition of the 2D-STE variables were determined by performing 30 examination by the same observer (AC) on 5 healthy awake dogs, randomly selected from the control group, on two different days over a one-week period. On a given day all the dogs were examined at 3 non-consecutive times (therefore a total of 15 2D-STE examination were performed per day).

The intra-operator between-day variability for measurements of the 2D-STE variables was determined measuring the same 5 examination (1 study of each dog) repeatedly on two different days over a one-week period.

2D-STE examinations were performed as previously described. All images and loops were stored and analysed off-line. The mean and SD values resulting from post processing of repeated examination of dogs were used for calculation the between day and within-day operator Coefficient of Variation (CV%).

CV was calculated as follows:

$$CV = (SD/mean) \times 100$$

The degree of variability was defined as:

CV < 5%, very low variability;

5-15%, low variability;

16-25% moderate variability;

> 25%, high variability[158].

3.4 Statistical analysis

Shapiro-Wilk normality test was used to assess the normal distribution of the collected variables. Mean and standard deviation (SD) were used as measures of central tendency and variability to describe quantitative variables. We used Student's t-test to assess differences between control and SIRS groups. Pearson correlations between continuous variables were performed. When the variables were not normally distributed, we used the Spearman's method to correlate them. Statistical significance was considered when the p-value was less than 0,05. However, that value was modified according to the Bonferroni's formula in case of multiple comparisons. Statistical analyses were performed using STATA13 (StataCorp, College Station, TX, USA).

The coefficient of correlation *r* was interpreted as follows[159]:

***r* value**	**Interpretation**
0,9 to 1 (-0,9 to -1)	Very high positive (negative) correlation
0,7 to 0,9 (-0,7 to -0,9)	High positive (negative) correlation
0,5 to 0,7 (-0,5 to -0,7)	Moderate positive (negative) correlation
0,3 to 0,5 (-0,3 to -0,5)	Low positive (negative) correlation
0 to 0,3 (0 to -0,3)	Negligible correlation

4. RESULTS

40 dogs were initially enrolled in the study. 22 dogs in the SIRS group and 18 in the control group. At a later stage 5 dogs of the SIRS group, although responded to the SIRS criteria, were excluded because they had serum CRP levels within normal limits. One dog from the control group was excluded because he had leucocytosis and serum CRP levels above the reference range.

Finally 34 dogs, 17 for each group were included:

- **SIRS group** was composed of 17 dogs, 13 female (4 female spayed) and 4 male (2 male castrated), with mean age of 7 ± 3,5 years and mean weight of 22,94 ± 11,49 Kg, composed of 7 Mongrel dogs, 2 German Shepherd, 2 Cane Fonnese, 1 Labrador Retriever, 1 English Setter, 1 Cane Corso, 1 Shi Tzu, 1 Espagneul Breton and 1 Staffordshire Bull Terrier; Dogs of SIRS group were presented for a variety of underlying conditions as listed in Table 1. Median duration of clinical signs before admission as noted by the owners was 5,7 days (range 1-30 days). No dog, in this group, showed symptoms of severe shock like bradycardia, hypothermia, hypotension, stupor or coma. All dogs, of the SIRS group, improved during the hospitalization period and survived until the discharge.
- **Control group** were composed of 17 dogs, 7 female (3 female spayed) and 10 male (4 male castrated), with mean age of 5,2 ± 2,4 years composed of 7 Mongrel dogs, 3 Labrador Retriever, 3 English Setter, 2 Staffordshire Bull Terrier, 1 Dachshund and 1 Beagle.

Signalment, clinical condition, CRP and cTnI levels recorded for each dog are illustrated in Table 1 (SIRS group) and in Table 2 (control group). All the 34 dogs had blood pressure values within the normal limits [148] (data not showed), no dog had persistent arrhythmias during the echocardiographic examination.

Table 1
Signalment, diagnosis, SIRS criteria, CRP and cTnI levels, and ECG of the dogs included in the SIRS group.

N	SEX	BREED	AGE Months	WEIGHT Kg	DIAGNOSIS	WBC/µl	Body temp (°C)	Heart rate (beats/min)	Respiratory rate (breaths/min)	SIRS	CRP mg/dl	TnI ng/ml	ECG
P13	MC	MONGREL	96	27	IMMUNE-MEDIATED THROMBOCYTOPENIA	3500	40	110	60	Yes	2,98	0,039	S
P14	F	GERMAN SHEPHERD	72	28	SYSTEMIC LUPUS ERYTHEMATOSUS	8480	41	130	46	Yes	3,93	0,120	S
P23	FS	MONGREL	36	13	ENTERITIS	39950	38,7	122	40	Yes	7,43	0,103	S
P10	FS	MONGREL	96	14	PANCREATITIS	5670	39	174	50	Yes	37,26	0,326	S + VPC
P04	M	GERMAN SHEPHERD	96	42	SPLENIC/HEPATIC HEMANGIOSARCOMA	26200	38	132	50	Yes	8,21	0,040	S + VPC
P15	MC	MONGREL	156	35	METASTATIC MAST CELL TUMOR	34360	39,7	128	58	Yes	6,53	0,041	S
P16	F	ENGLISH SETTER	144	11	ULCERATED MAMMARY CARCINOMA	42330	39,8	128	42	Yes	16,25	0,062	S + VPC
P01	FS	MONGREL	36	10	LEISHMANIOSIS	16410	39,3	94	44	Yes	9,37	0,042	S
P17	MC	MONGREL	72	26	EHRLICHIOSIS	27780	39,5	166	52	Yes	21,71	0,038	S + VPC
P19	FS	CANE FONNESE	36	22	EHRLICHIOSIS	35360	39,6	165	44	Yes	8,35	0,045	S
P21	F	CANE CORSO	18	33	EHRLICHIOSIS	22810	40,07	92	28	Yes	9,64	0,036	S
P22	F	CANE FONNESE	144	32	ENDOMETRITIS	9340	39,3	160	46	Yes	18,71	0,054	S
P02	F	LABRADOR RETRIEVER	60	40	PYOMETRA	30570	39	104	40	Yes	21,18	0,030	S
P11	F	MONGREL	84	18	PYOMETRA	17470	39,8	119	40	Yes	19,56	0,037	S
P24	F	SHIH TZU	96	4	PYOMETRA	13290	38,8	193	38	Yes	9,60	0,035	S
P18	F	EPAGNEUL BRETON	60	9	PYOMETRA	41440	39,9	70	42	Yes	14,04	0,086	S
P06	F	STAFFORDSHIRE BULL TERRIER	144	26	PYOMETRA	15000	38,5	86	48	Yes	10,77	0,033	S

Abbreviations: M, male; MC, male castrated; F, female; FS, female spayed; S, sinusal rhythm; VPC presence of ventricular premature complex. The numbers highlighted in yellow are the positive SIRS criteria.

Table 2
Signalment, SIRS criteria, CRP and cTnI levels and ECG of the dogs included in the control group.

N	SEX	BREED	AGE Months	WEIGHT Kg	WBC/µl	Body temp (°C)	Heart rate (beats/min)	Respiratory rate (breaths/min)	SIRS	CRP mg/dl	TnI ng/ml	ECG
N01	F	LABRADOR RETRIEVER	84	37	7100	38,5	93	30	No	0,340	0,061	S
N02	M	LABRADOR RETRIEVER	72	45	8800	38,6	97	26	No	0,003	0,040	S
N03	F	LABRADOR RETRIEVER	36	36	8650	38,5	98	24	No	nd	0,042	S
N04	F	ENGLISH SETTER	84	23	9280	38,3	113	20	No	0,414	0,040	S
N05	M	ENGLISH SETTER	24	19	10240	38,8	83	22	No	0,013	0,036	S
N07	M	BEAGLE	36	20	6120	39	80	24	No	0,199	0,058	S
N09	F	STAFFORDSHIRE BULL TERRIER	18	17	10850	38,8	105	20	No	0,020	0,043	S
N10	MC	MONGREL	96	20	11360	38,2	122	22	No	nd	0,037	S
N11	MC	STAFFORDSHIRE BULL TERRIER	120	28	6750	38,5	112	20	No	nd	0,042	S
N12	FS	MONGREL	84	7	7120	38,6	110	26	No	0,011	0,057	S
N14	M	DACHSHUND	84	9	7100	38,7	132	24	No	nd	0,097	S
N15	MC	MONGREL	24	17	8860	38,4	110	22	No	nd	0,072	S
N17	M	MONGREL	48	5	7400	39,2	92	28	No	nd	0,051	S
N19	FS	MONGREL	72	8	8600	38,8	148	26	No	nd	0,070	S
N20	FS	MONGREL	72	9	7870	39	112	24	No	0,280	0,059	S
N21	MC	MONGREL	48	8	9840	38,7	117	30	No	nd	0,054	S
N06	M	ENGLISH SETTER	60	17	7500	38,6	70	18	No	0,138	0,058	S

Abbreviations: M, male; MC, male castrated; F, female; FS, female spayed; S, sinusal rhythm; VPC presence of ventricular premature complex; nd, not detected.

4.1 Signalment

Mean age, weight and sex were not significantly different between the two groups as shown in Table 3.

Table 3
Age, sex and weight difference between the SIRS and control group

Variables	Control group	SIRS group	*p-value*
Weight (Kg), mean (SD)	19.12 (11.68)	22.94 (11.49)	0.34
Age (months), mean (SD)	62.47 (28.86)	85.06 (42.76)	0.08
Male, n(%)	10 (58.8)	4 (23.5)	0.08

4.2 Mean CRP, cTnI and Heart Rate

As expected, CRP serum level and HR were significant higher in the SIRS group than in the control group (Table 4). Dogs with SIRS had mean cTnI serum level higher than healthy dogs but the difference, was not significant (Table 4 and Figure 8).

Table 4
Mean CRP, TnI serum levels and heart rate difference between SIRS and control group.

Variables	Control group	SIRS group	*p-value*
CRP (mg/dl), mean (SD)	**0,158 (0,159)**	**13,27 (8,51)**	**0.0001**
HR (bpm), mean (SD)	**105.53 (19.33)**	**127.82 (34.27)**	**0.03**
cTnI (ng/ml), mean (SD)	0,054 (0,016)	0,069 (0,071)	0.41

CRP, C-Reactive Protein; HR, Heart Rate; cTnI, Cardiac Troponin I; SD, Standard Deviation. Highlighted in yellow the variables significantly different between the two groups.

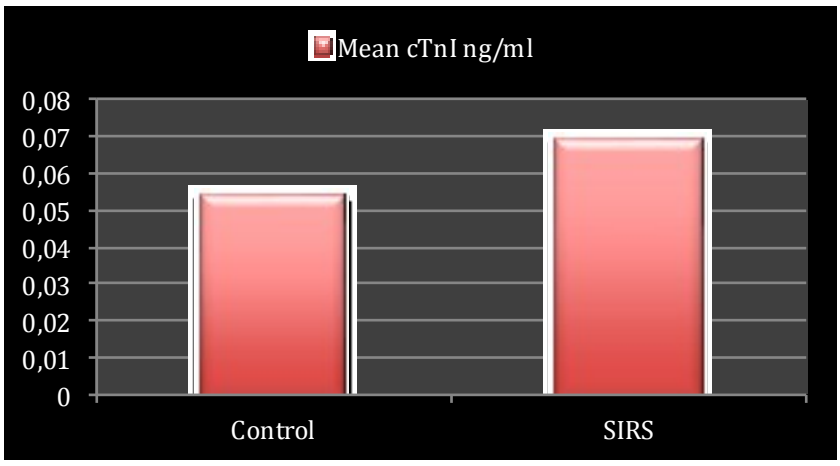

Figure 8. Graphic comparison of mean cTnI (ng/ml) serum level between the two groups

4.3 2D, M-Mode and Doppler derived indices of LV systolic function

2-Dimensional, M-mode and Doppler derived indices of LV systolic function are shown in Table 5 (SIRS group) and in Table 6 (control group).

Table 5
2-Dimensional, M-mode and Doppler measurements and derived index of systolic function of the SIRS group

N	LV EDV(ml) Simpson	LV ESV(ml) Simpson	EF% Simpson	LA cm	Ao cm	LA/Ao	IVSd cm	LVIDd cm	LVPWd cm	IVSs cm	LVIDs cm	LVPWs cm	LV EDV(ml) Teicholz	LV ESV(ml) Teicholz	EF% Teicholz	FS %	PEP ms	ET ms	PEP/ET
P13	29,9	12,5	58	2,37	1,84	1,28	0,92	3,06	0,92	1,44	1,81	1,25	36,7	9,8	73	41	70	150	0,46
P14	48,1	16,2	66	3	2,43	1,23	1,29	3,86	1,01	1,62	2,42	1,56	64,3	20,5	68	37	77	116	0,66
P23	36,6	19,8	46	2,83	1,98	1,43	0,87	3,53	0,97	1,04	2,43	1,35	51,9	20,7	60	31	91	148	0,61
P10	19,9	7,8	61	1,92	1,79	1,07	1,03	3,03	0,83	1,29	2	0,99	35,8	12,7	65	34	54	116	0,46
P04	83,1	40,8	51	3,28	2,67	1,23	1,04	4,83	0,9	1,38	3,1	1,49	109,2	37,9	65	36	74	188	0,39
P15	36,9	15,9	57	3,38	2,5	1,35	0,86	3,06	0,92	1,21	2,02	1,53	36,7	13,0	64	34	68	155	0,43
P16	35,1	15,4	56	2,59	1,81	1,43	0,65	3,35	0,77	0,74	2,26	1	45.7	17,3	62	33	75	148	0,5
P01	26,4	16,2	39	2,18	1,52	1,43	0,86	3,27	0,79	0,82	2,39	1,09	43,3	19,9	54	27	65	180	0,36
P17	22,1	9,1	59	2,32	2,3	1,01	1,24	2,6	1,09	1,47	1,58	1,51	24,6	6,9	72	39	59	113	0,52
P19	39,3	14,6	63	2,31	2,02	1,14	1,02	3,32	0,94	1,28	2,14	1,59	44,7	15,1	66	35	72	136	0,52
P21	58,3	19,8	66	2,36	2,22	1,06	0,91	3,77	0,96	1,46	2,39	1,41	60,7	19,9	67	36	57	155	0,36
P22	59,1	31,9	46	2,93	2,43	1,21	1,12	4,1	1,06	1,42	2,95	1,34	74,2	33,5	55	28	88	131	0,67
P02	74,4	41	45	2,91	2,62	1,11	0,98	4,05	1,16	1,55	2,87	1,57	71,9	31,3	56	29	104	174	0,59
P11	28,3	15,8	44	2,42	1,68	1,44	0,83	3,21	0,78	1,1	2,2	1,17	41,2	16,2	61	31	84	168	0,5
P24	3,1	1,4	55	1,28	1,35	1,08	0.59	1,21	0,73	0,67	0,73	0,77	3,4	0,9	75	40	60	116	0,51
P18	25,2	7,6	70	1,84	1,7	1,09	0,82	3,27	0,72	1,27	1,79	1,19	43,1	9,5	78	45	73	157	0,46
P06	60,7	31,8	48	2,56	2,37	1,08	0,92	3,61	1,29	1,3	2,63	1,51	54,8	25,4	54	27	86	177	0,48

Highlighted in yellow the values below the reference range.

Table 6
2-Dimensional, M-mode and Doppler measurements and derived index of systolic function of the control group

N	LV EDV(ml) Simpson	LV ESV(ml) Simpson	EF% Simpson	LA cm	Ao cm	LA/Ao	IVSd cm	LVIDd cm	LVPWd cm	IVSs cm	LVIDs cm	LVPWs cm	LV EDV(ml) Teicholz	LV ESV(ml) Teicholz	EF% Teicholz	FS %	PEP ms	ET ms	PEP/ET
N01	65,5	31,6	52	3,56	2,82	1,26	1,07	4,27	1,15	1,46	2,88	1,48	81,7	31,7	61	33	72	196	0,36
N02	72,4	33,6	54	3,35	2,38	1,40	1,54	4,38	1,12	2,1	3,01	1,62	87,0	35,2	60	31	88	186	0,47
N03	68	29,7	56	3,09	2,31	1,33	0,83	4,64	0,81	1,36	3,21	1,31	68,0	29,7	58	31	100	190	0,52
N04	43	13,5	69	2,43	2,11	1,15	1,04	3,96	1,04	1,46	2,62	1,2	68,3	25,0	63	34	70	154	0,45
N05	41,7	21	50	2,63	2,16	1,21	0,93	3,79	0,84	1,21	2,55	1,09	61,7	23,5	62	33	72	164	0,43
N07	48,6	15,4	68	2,87	1,97	1,45	0,89	3,5	1,21	1,23	2,23	1,75	50,8	16,8	67	36	74	186	0,39
N09	41	14,6	64	2,3	1,90	1,21	1,05	4.08	0,89	1,36	2,77	1,11	73,4	28,9	61	32	69	177	0,38
N10	29,4	13	56	2,26	1,74	1,30	0,77	3,15	0,82	1,24	2,02	1,29	39,5	13,0	67	36	74	174	0,42
N11	54,3	23,4	57	2,47	2,13	1,16	1,08	4,31	1,01	1,35	2,88	1,4	83,3	31,6	62	33	85	180	0,47
N12	10,6	4,3	59	1,59	1,28	1,24	0,84	2,16	0,75	1,06	1,56	0,82	15,4	6,7	57	28	65	172	0,37
N14	24,5	8,8	64	1,7	1,40	1,21	0,61	3,16	0,69	0,88	2,03	1,02	39,7	13,2	67	36	61	170	0,35
N15	42,3	15,6	63	2,29	1,79	1,28	0,82	3,95	0,93	1,36	2,67	1,29	68,1	26,3	61	33	69	184	0,37
N17	11	4,8	56	1,5	1,21	1,24	0,65	2,37	0,65	0,75	1,59	0,9	19,5	7,0	64	33	63	184	0,34
N19	20,9	7	66	1,95	1,77	1,10	0,9	2,73	0,82	1,22	1,58	1,22	27,7	6,9	75	42	61	148	0,41
N20	20,2	8,8	56	2	1,83	1,10	0,67	3,37	0,57	0,9	2,35	0,8	46,4	19,1	59	30	72	172	0,41
N21	14,6	5,4	63	1,9	1,70	1,11	0,73	2,37	0,76	0,89	1,78	1,03	19,5	9,4	52	25	61	144	0,42
N06	46,5	19,5	58	2,5	1,96	1,27	0,74	4	0,72	1,11	2,62	1,12	70,1	25,2	64	34	78	190	0,41

4 dogs in the SIRS group had LV systolic and diastolic diameters below the reference limits[152], which is suggestive of hypovolemia. Mean EF% calculated by the Monoplane Simpson Method of Disks, mean EF% calculated using the Teicholz formula and the Doppler derived Pre-Ejection Period (PEP) didn't show significant difference between SIRS and control group. In both groups the mean values are within the normal limits[115, 160]. On the other hand, the mean Ejection Time (ET) of the SIRS group resulted significant lower compared to the control group, therefore the ratio PEP/ET were significantly higher and above the reference range[160] in the SIRS group (Table 7 and Figure 9).

Table 7
Mean and SD values of 2D, M-mode and Doppler derived indices of LV systolic function, and differences between the two groups

Variables	Control group		SIRS group		*p-value*
	Mean	±SD	Mean	±SD	
EF% Simpson	59,47	5,61	54,71	9,01	0,07
EF % Teicholz	62,35	5,05	64,41	7,35	0,35
FS %	32,94	3,68	34,29	5,16	0,39
PEP ms	72,59	10,49	73,94	13,43	0,75
ET ms	**174,76**	15,04	**148,71**	24,30	**0,0007**
PEP/ET	**0,41**	0,05	**0,50**	0,09	**0,001**

Highlighted in yellow the variables significantly different between the two groups.

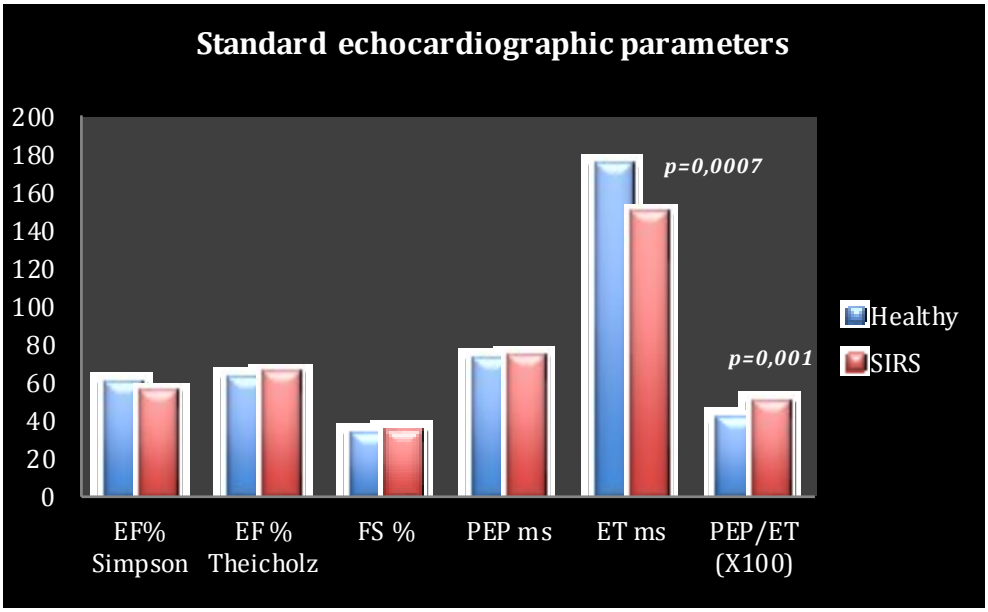

Figure 9. Graphic comparison of mean 2D, M-mode and Doppler derived indices of LV systolic function between SIRS and control group

4.4 Mean EF% obtained by Speckle Tracking method

The EF% obtained with the Speckle Tracking Echocardiography (STE EF%), calculated by the XStrain-4D software, revealed a significant difference between the SIRS and control group. Dogs with systemic inflammation showed a significantly lower STE EF% compared to the control group (Table 8A and Figure 10).

Table 8A
Mean EF% values calculated by the three methods and differences between the two groups

Variables	Control group		SIRS group		*p-value*
	Mean	±SD	Mean	±SD	
EF% Simpson	59,47	5,61	54,71	9,01	0,07
EF % Teicholz	62,35	5,05	64,41	7,35	0,35
STE EF %	**53.2**	**8.4**	**43.9**	**8.4**	**0.003**

Highlighted in yellow the variables significantly different between the two groups.

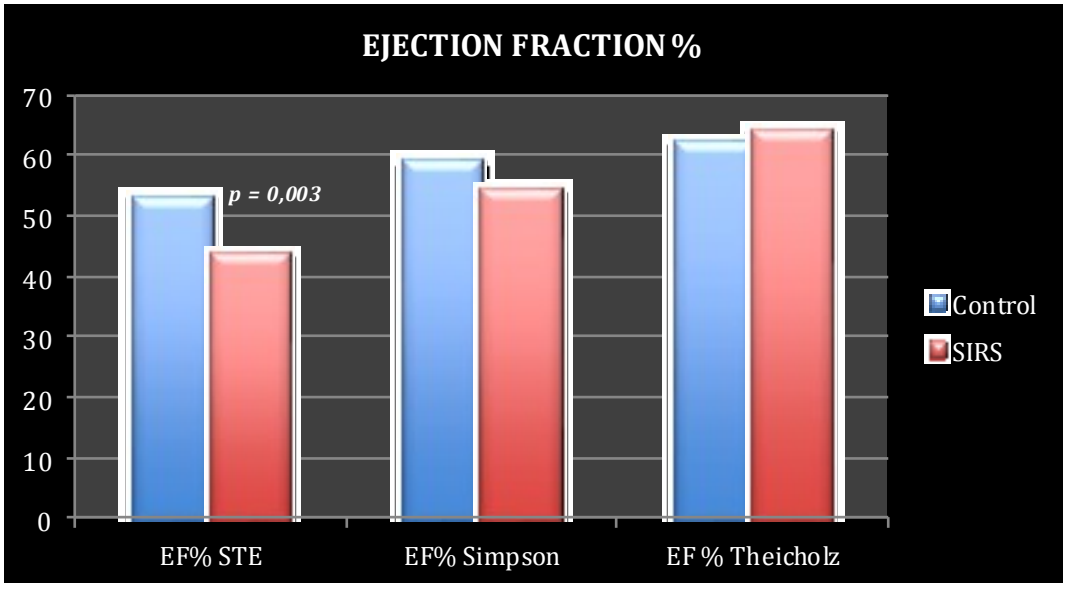

Figure 10. Graphic comparison of the EF% calculated by three echocardiographic methods between the two groups

4.5 Speckle Tracking endocardial variables

Endocardial (ENDO) systolic peak transversal displacement and velocity of displacement were not significantly different between SIRS and control group (Table 8B). In the same way, peak longitudinal ENDO velocity of displacement and Strain Rate did not differ significantly between SIRS and control group (Table 8B). Otherwise, the systolic ENDO regional and Global Peak Longitudinal Strain (ENDO GLPS) and displacement were significantly lower in the SIRS group compared to the normal controls (Table 8B).

Table 8B
Values of mean regional and global endocardial STE variables, differences between the two groups

Variables	Control		SIRS		*p-value*
	Mean	SD	Mean	SD	
Peak transversal displacement ENDO global value (mm)	4,28	1,44	3,47	1,13	0,08
Peak transversal displacement ENDO global basal level (mm)	4,88	1,43	4,19	1,39	0,16
Peak transversal displacement ENDO global mid-level (mm)	4,58	1,53	3,75	1,30	0,08
Peak transversal displacement ENDO global apical level (mm)	3,39	1,52	2,50	1,06	0,06
Peak longitudinal displacement ENDO global value (mm)	**4,05**	**1,02**	**3,25**	**0,96**	**0,03**
Peak longitudinal displacement ENDO global basal level (mm)	**5,93**	**1,71**	**4,79**	**1,27**	**0,03**
Peak longitudinal displacement ENDO global mid-level (mm)	**4,25**	**1,07**	**3,33**	**1,03**	**0,02**
Peak longitudinal displacement ENDO global apical level (mm)	1,98	0,65	1,64	0,76	0,17
Peak longitudinal strain rate ENDO global value (1/s)	-1,87	0,32	-1,70	0,40	0,17
Peak longitudinal strain rate ENDO global basal level (1/s)	-1,84	0,36	-1,78	0,40	0,64
Peak longitudinal strain rate ENDO global mid-level (1/s)	-1,87	0,43	-1,65	0,41	0,12
Peak longitudinal strain rate ENDO global apical level (1/s)	-1,95	0,37	-1,66	0,56	0,09
Peak longitudinal strain ENDO global value (%)	**-18,54**	**4,08**	**-14,60**	**3,17**	**0,004**
Peak longitudinal strain ENDO global basal level (%)	**-17,48**	**4,85**	**-14,44**	**3,13**	**0,04**
Peak longitudinal strain ENDO global mid-level (%)	**-18,38**	**4,31**	**-14,40**	**3,13**	**0,004**
Peak longitudinal strain ENDO global apical level (%)	**-19,75**	**4,16**	**-14,99**	**4,45**	**0,003**
Peak transversal velocity ENDO global value (cm/sec)	4,25	1,21	3,77	1,03	0,22
Peak transversal velocity ENDO global basal level (cm/sec)	5,01	1,12	4,69	1,29	0,44
Peak transversal velocity ENDO global mid-level (cm/sec)	4,50	1,39	3,91	1,09	0,18
Peak transversal velocity ENDO global apical level (cm/sec)	3,25	1,28	2,70	1,09	0,19
Peak longitudinal velocity ENDO global value (cm/sec)	4,02	0,76	3,76	0,85	0,36
Peak longitudinal velocity ENDO global basal level (cm/sec)	5,59	1,10	5,31	1,24	0,49
Peak longitudinal velocity ENDO global mid-level (cm/sec)	4,25	0,83	3,84	0,89	0,18
Peak longitudinal velocity ENDO global apical level (cm/sec)	2,22	0,60	2,12	0,68	0,68

Highlighted in yellow the variables significantly different between the two groups.

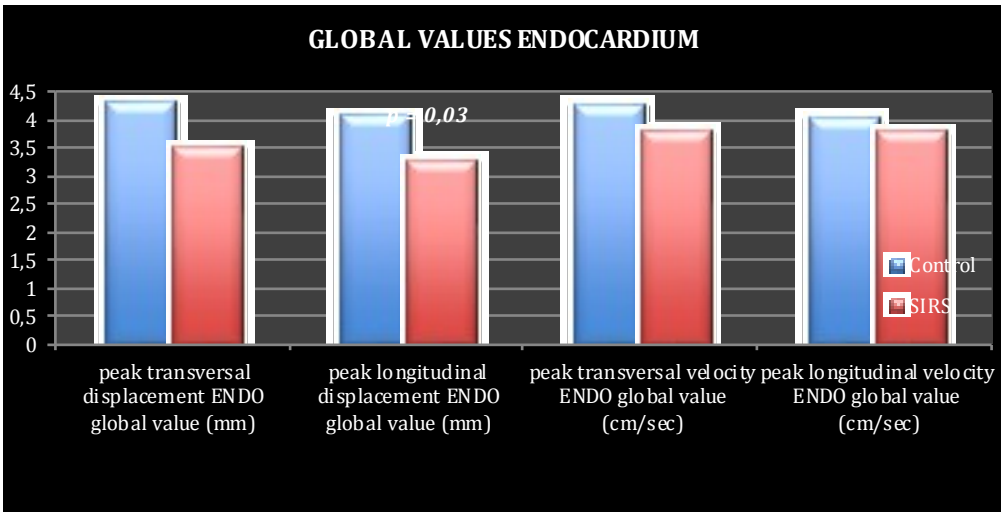

Figure 11. Graphic comparison of the mean global endocardial STE variables (displacement and velocity of displacement in longitudinal and transversal direction) between the two groups

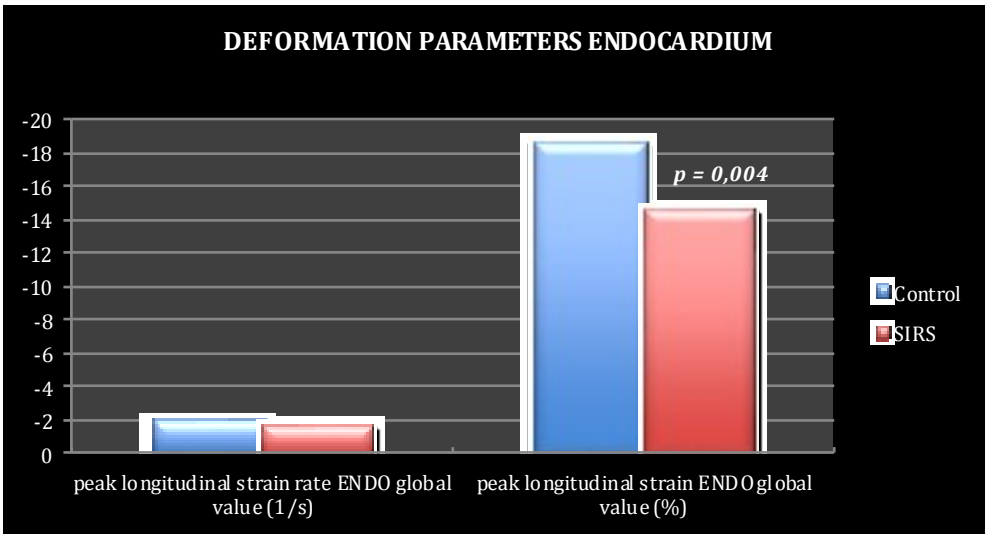

Figure 12. Graphic comparisons between mean global endocardial longitudinal parameters of deformation St and StR

4.6 Speckle Tracking epicardial variables

Only few, and not representative of the global LV deformation, epicardial (EPI) STE variables were statistically different between the two groups (Table 9).

Table 9
Mean values of regional and global epicardial STE variables, differences between the two groups

Variables	Healty		Disease		*p-value*
	Mean	SD	Mean	SD	
Peak transversal displacement EPI, global value (mm)	2,74	0,74	2,29	0,69	0,07
Peak transversal displacement EPI, global basal level (mm)	3,70	0,88	3,23	1,11	0,18
Peak transversal displacement EPI, global mid-level (mm)	2,89	0,93	2,44	0,78	0,14
Peak transversal displacement EPI, global apical level (mm)	**1,63**	**0,69**	**1,20**	**0,51**	**0,04**
Peak longitudinal displacement EPI global value (mm)	4,57	1,24	4,04	1,10	0,2
Peak longitudinal displacement EPI global basal level (mm)	7,20	2,11	6,53	1,83	0,33
Peak longitudinal displacement EPI global mid-level (mm)	4,63	1,19	3,96	1,09	0,1
Peak longitudinal displacement EPI global apical level (mm)	1,88	0,60	1,64	0,53	0,22
Peak longitudinal strain rate EPI global value (1/sec)	-1,62	0,29	-1,67	0,47	0,7
Peak longitudinal strain rate EPI global basal level (1/s)	-1,88	0,33	-2,05	0,56	0,28
Peak longitudinal strain rate EPI global mid-level (1/s)	-1,72	0,33	-1,80	0,52	0,6
Peak longitudinal strain rate EPI global apical level (1/s)	-1,25	0,28	-1,16	0,39	0,41
Peak longitudinal strain EPI global value (%)	-16,22	3,01	-15,03	4,11	0,34
Peak longitudinal strain EPI global basal level (%)	-18,41	3,85	-16,41	8,85	0,4
Peak longitudinal strain EPI global mid-level (%)	-17,48	3,13	-15,81	4,43	0,21
Peak longitudinal strain EPI global apical level (%)	**-12,77**	**2,69**	**-10,47**	**3,40**	**0,04**
Peak transversal velocity EPI global value (cm/sec)	3,01	0,95	2,88	0,64	0,64
Peak transversal velocity EPI global basal level (cm/sec)	4,03	1,02	3,81	0,81	0,5
Peak transversal velocity EPI global mid-level (cm/sec)	3,16	1,15	3,16	0,77	0,99
Peak transversal velocity EPI global apical level (cm/sec)	1,85	0,82	1,67	0,66	0,48
Peak longitudinal velocity EPI global value (cm/sec)	4,40	0,86	4,49	1,08	0,78
Peak longitudinal velocity EPI global basal level (cm/sec)	6,76	1,33	7,07	1,69	0,56
Peak longitudinal velocity EPI global mid-level (cm/sec)	4,57	0,92	4,45	1,07	0,74
Peak longitudinal velocity EPI global apical-level (cm/sec)	1,87	0,49	1,95	0,75	0,7

Highlighted in yellow the variables significantly different between the two groups.

4.7 Speckle Tracking transversal Strain and Strain rate variables

Mean values of transversal Strain and Strain Rate were lower in the SIRS group compared to the healthy controls but the difference was not statistically significant (Table 10 and Figure 13).

Table 10
Mean values STE transversal variables and differences between the two groups

Variables	Control		SIRS		*p-value*
	Mean	SD	Mean	SD	
Peak transversal strain rate global value (1/s)	2,75	0,58	2,51	0,42	0,18
Peak transversal strain rate global basal level (1/s)	3,17	0,54	2,97	0,59	0,32
Peak transversal strain rate global mid-level (1/s)	2,86	0,59	2,61	0,47	0,18
Peak transversal strain rate global apical level (1/sec)	2,23	0,70	1,96	0,54	0,21
Peak transversal strain global value (%)	27,00	10,68	22,13	6,82	0,12
Peak transversal strain global basal level (%)	28,95	10,65	24,56	8,22	0,19
Peak transversal strain global mid-level (%)	27,55	10,41	22,86	7,14	0,14
Peak transversal strain global apical level (%)	24,49	12,01	18,96	6,81	0.11

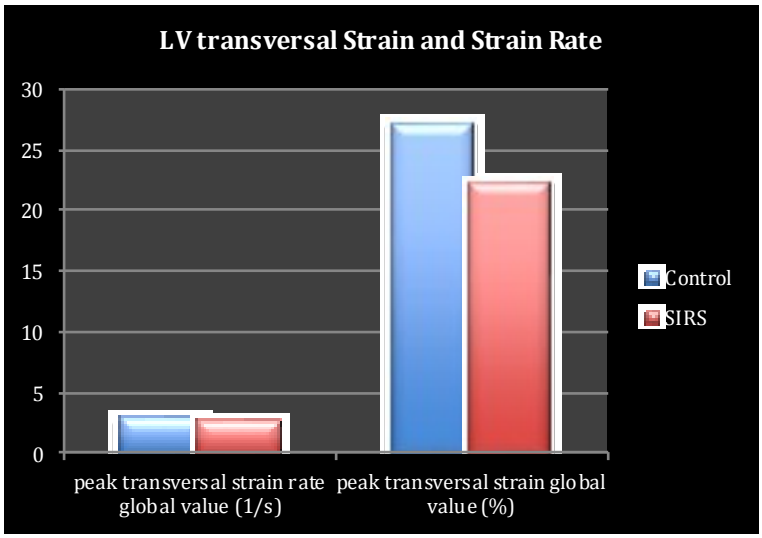

Figure 13. Graphic comparison of the mean global transversal Strain and Strain Rate between the two groups

4.8 Variability study

The intra-operator within day and between-day variability for acquisition of the STE variables were considered low because mean CV = 12% (minimum 6% and maximum 21%). The intra-operator between-day variability for measurements of the STE variables was considered low because mean CV = 9% (minimum 4% and maximum 15%).

4.9 Correlation between variables

To understand the link between inflammation, myocardial injury and myocardial dysfunction, we analysed the correlations between the CRP and cTnI levels and between STE variables and CRP, cTnI in the SIRS group:

- In our study there was a negligible *(r=-0,15)* and not significant *(p=0,58)* negative correlation between CRP and cTnI serum levels in the SIRS group;
- There was a low *(r < 0,5)* and not significant *(p>0,05)* correlation between STE variables and CRP levels (Table 11 and 12);
- There was a moderate positive *(r = 0,53)* and significant *(p = 0,028)* correlation between Global Peak Longitudinal EPI Strain Rate and cTnI levels (Table 11);
- There was a moderate positive *(r = 0,55)* and significant *(p = 0,021)* correlation between Global Peak Longitudinal EPI velocity of displacement and cTnI levels (Table 11);
- There was a moderate positive *(r = 0,56)* and significant *(p = 0,017)* correlation between Global Peak Longitudinal ENDO velocity of displacement and cTnI levels (Table 12);

Table 11
Linear correlation between epicardial STE variables, CRP and cTnI serum levels in the SIRS group expressed by the Pearson's coefficient of correlation *(r-value)* and significance level of the correlation *(p-value)*

Variables	CRP mg/dl		cTnI ng/ml	
	(r value)	***p-value***	**(*r value*)**	***p-value***
Speck track EF % STE	0.1072	*0.6822*	0.1571	*0.5470*
Peak transversal displacement EPI, global value (mm)	0.0748	*0.7755*	-0.0940	*0.7197*
Peak transversal displacement EPI, global basal level (mm)	0.0016	*0.9952*	-0.0244	*0.9259*
Peak transversal displacement EPI, global mid-level (mm)	0.1183	*0.6512*	-0.1762	*0.4987*
Peak transversal displacement EPI, global apical level (mm)	0.1263	*0.6292*	-0.0575	*0.8266*
Peak longitudinal displacement EPI global value (mm)	-0.0137	*0.9583*	0.2005	*0.4404*
Peak longitudinal displacement EPI global basal level (mm)	-0.0640	*0.8071*	0.1636	*0.5304*
Peak longitudinal displacement EPI global mid-level (mm)	-0.0269	*0.9183*	0.1550	*0.5526*
Peak longitudinal displacement EPI global apical level (mm)	0.1976	*0.4472*	0.3730	*0.1403*
Peak longitudinal strain rate EPI global value (1/sec)	0.3092	*0.2272*	0.5304	*0.0285*
Peak longitudinal strain rate EPI global basal level (1/s)	0.3731	*0.1402*	0.6080	*0.0096*
Peak longitudinal strain rate EPI global mid-level (1/s)	0.3051	*0.2337*	0.4753	*0.0538*
Peak longitudinal strain rate EPI global apical level (1/s)	0.1796	*0.4904*	0.4280	*0.0865*
Peak longitudinal strain EPI global value (%)	0.1364	*0.6015*	0.3299	*0.1960*
Peak longitudinal strain EPI global basal level (%)	0.1943	*0.4550*	0.3277	*0.1991*
Peak longitudinal strain EPI global mid-level (%)	0.1729	*0.5070*	0.3434	*0.1772*
Peak longitudinal strain EPI global apical level (%)	0.1334	*0.6097*	0.2329	*0.3682*
Peak transversal velocity EPI global value (cm/sec)	0.0697	*0.7904*	0.1005	*0.7012*
Peak transversal velocity EPI global basal level (cm/sec)	0.0838	*0.7491*	0.0932	*0.7219*
Peak transversal velocity EPI global mid-level (cm/sec)	0.1052	*0.6879*	0.1241	*0.6351*
Peak transversal velocity EPI global apical level (cm/sec)	-0.0264	*0.9198*	0.0273	*0.9172*
Peak longitudinal velocity EPI global value (cm/sec)	0.1873	*0.4717*	0.5529	*0.0213*
Peak longitudinal velocity EPI global basal level (cm/sec)	0.0643	*0.8062*	0.4097	*0.1025*
Peak longitudinal velocity EPI global mid-level (cm/sec)	0.1585	*0.5435*	0.5428	*0.0244*
Peak longitudinal velocity EPI global apical-level (cm/sec)	0.4301	*0.0848*	0.6784	*0.0028*

Highlighted in yellow the variables significantly correlated between them.

Table 12
Linear correlation between endocardial STE variables, CRP and cTnI serum levels in the SIRS group expressed by the Pearson's coefficient of correlation *(r-value)* and significance level of the correlation *(p-value)*

Variables	CRP mg/dl		cTnI ng/ml	
	(r value)	*p-value*	*(r value)*	*p-value*
Peak transversal displacement ENDO global value (mm)	-0.0826	*0.7526*	-0.2321	*0.3700*
Peak transversal displacement ENDO global basal level (mm)	-0.1708	*0.5121*	-0.1544	*0.5542*
Peak transversal displacement ENDO global mid-level (mm)	0.0055	*0.9834*	-0.3076	*0.2298*
Peak transversal displacement ENDO global apical level (mm)	-0.0485	*0.8532*	-0.1751	*0.5013*
Peak longitudinal displacement ENDO global value (mm)	-0.0654	*0.8030*	0.1987	*0.4444*
Peak longitudinal displacement ENDO global basal level (mm)	-0.1010	*0.6997*	0.0897	*0.7322*
Peak longitudinal displacement ENDO global mid-level (mm)	-0.0990	*0.7054*	0.1643	*0.5286*
Peak longitudinal displacement ENDO global apical level (mm)	0.0592	*0.8215*	0.3867	*0.1252*
Peak longitudinal strain rate ENDO global value (1/s)	0.1564	*0.5490*	0.3185	*0.2128*
Peak longitudinal strain rate ENDO global basal level (1/s)	0.0978	*0.7088*	0.1610	*0.5371*
Peak longitudinal strain rate ENDO global mid-level (1/s)	0.2160	*0.4049*	0.2482	*0.3367*
Peak longitudinal strain rate ENDO global apical level (1/s)	0.1170	*0.6546*	0.4019	*0.1098*
Peak longitudinal strain ENDO global value (%)	0.0540	*0.8369*	0.0865	*0.7414*
Peak longitudinal strain ENDO global basal level (%)	0.0872	*0.7394*	0.0444	*0.8655*
Peak longitudinal strain ENDO global mid-level (%)	0.0296	*0.9102*	-0.0273	*0.9172*
Peak longitudinal strain ENDO global apical level (%)	0.0284	*0.9139*	0.1714	*0.5108*
Peak transversal velocity ENDO global value (cm/sec)	0.0662	*0.8007*	0.0242	*0.9266*
Peak transversal velocity ENDO global basal level (cm/sec)	-0.0256	*0.9224*	0.0453	*0.8628*
Peak transversal velocity ENDO global mid-level (cm/sec)	0.1497	*0.5664*	-0.0324	*0.9017*
Peak transversal velocity ENDO global apical level (cm/sec)	0.0640	*0.8072*	0.0464	*0.8595*
Peak longitudinal velocity ENDO global value (cm/sec)	0.1879	*0.4701*	0.5687	*0.0172*
Peak longitudinal velocity ENDO global basal level (cm/sec)	0.0741	*0.7773*	0.4604	*0.0629*
Peak longitudinal velocity ENDO global mid-level (cm/sec)	0.1574	*0.5463*	0.5227	*0.0313*
Peak longitudinal velocity ENDO global apical level (cm/sec)	0.3678	*0.1464*	0.6242	*0.0074*

Highlighted in yellow the variables significantly correlated between them.

Table 13
Linear correlation between transversal STE variables, CRP and cTnI serum levels in the SIRS group expressed by the Pearson's coefficient of correlation *(r-value)* and significance level of the correlation *(p-value)*

Variables	CRP mg/dl		cTnI ng/ml	
	(r value)	*p-value*	(r value)	*p-value*
Peak transversal strain rate global value (1/s)	-0.0414	*0.8746*	0.1463	*0.5753*
Peak transversal strain rate global basal level (1/s)	-0.0744	*0.7766*	0.2045	*0.4310*
Peak transversal strain rate global mid-level (1/s)	-0.0601	*0.8188*	0.0483	*0.8540*
Peak transversal strain rate global apical level (1/sec)	0.0377	*0.8857*	0.0790	*0.7632*
Peak transversal strain global value (%)	-0.1196	*0.6476*	-0.1409	*0.5896*
Peak transversal strain global basal level (%)	-0.1496	*0.5665*	-0.1025	*0.6954*
Peak transversal strain global mid-level (%)	-0.1186	*0.6504*	-0.1556	*0.5509*
Peak transversal strain global apical level (%)	-0.0542	*0.8364*	-0.1369	*0.6004*

We analysed also the correlations between the echocardiographic variables measured in the SIRS group.

- EF% calculated with the Speckle Tracking software XStrain-4D™ had a high positive and significant correlation with the systolic Peak Longitudinal ENDO regional and Global Strain and displacement as shown in Table 14;

Table 14
Linear correlation between STE EF% and longitudinal endocardial variables in the SIRS group expressed by the Pearson's coefficient of correlation *(r-value)* and significance level of the correlation *(p-value)*

Variables	STE EF%	
	r-value	*p-value*
Peak longitudinal displacement ENDO global value (mm)	0.7434	0.0006
Peak longitudinal displacement ENDO global basal level (mm)	0.7896	0.0002
Peak longitudinal displacement ENDO global midlevel (mm)	0.6670	0.0034
Peak longitudinal displacement ENDO global apical level (mm)	0.5944	0.0119
Peak longitudinal strain ENDO global value (%)	0.7042	0.0016
Peak longitudinal strain ENDO global basal level (%)	0.5013	0.0404
Peak longitudinal strain ENDO global midlevel (%)	0.5628	0.0187
Peak longitudinal strain ENDO global apical level (%)	0.7566	0.0004

Highlighted in yellow the variables significantly correlated between them.

- A negligible negative *(r=-0,30)* and not significant *(p=0,24)* correlation was found between 2D STE EF% and the Doppler-derived index of systolic function PEP/ET in the SIRS group.

- Finally, to assess the influence of heart rate (HR) on Doppler-derived systolic time intervals we analysed the correlation between them in both groups.

- It was found a low positive and not significant correlation between Doppler derived PEP/ET and heart rate (HR) in both groups (Table 15);

Table 15
Correlation between PEP/ET and HR expressed by the Pearson's coefficient of correlation *(r-value)* and significance level of the correlation *(p-value)*

PEP/ET vs HR	*r-value*	*p-value*
Control group	0.08	0.77
SIRS group	0.38	0.13

- It was found a low negative and not significant correlation between Doppler derived PEP and heart rate (HR) in both groups (Table 16);

Table 16
Correlation between PEP and HR expressed by the Pearson's coefficient of correlation *(r-value)* and significance level of the correlation *(p-value)*

PEP vs HR	*r-value*	*p-value*
Control group	-0.41	0.11
SIRS group	-0.32	0.20

- On the contrary, there was a high negative and significant correlation between Doppler derived ET and heart rate (HR) in both groups (Table 17);

Table 17
Correlation between ET and HR expressed by the Pearson's coefficient of correlation *(r-value)* and significance level of the correlation *(p-value)*

ET vs HR	*r-value*	*p-value*
Control group	-0.69	0.002
SIRS group	-0.72	0.001

Highlighted in yellow the variables significantly correlated between them.

5. DISCUSSION

Myocardial dysfunction during SIRS and sepsis has been previously demonstrated in dogs[111] and humans[161]. Moreover, it has been shown that endotoxin and interleukins have a negative inotropic effect on ventricular myocites[82]. In the present study, as previously observed by Gommeren et al[112], dogs suffering from SIRS had standard echocardiographic parameters of LV systolic function, as Fractional Shortening (FS%) and Ejection Fraction (EF%), within the normal limits (Table 5). The mean FS% and EF% values were not statistically different between healthy dogs and dogs with SIRS *(p>0,05)*. In contrast to our findings, others studies[107, 119] found decrease FS% and EF% in dogs with various inflammatory conditions. The difference of our results could be due to the less severity of the underlying disease in our SIRS population, in fact, in our study, no dog presented severe shock at the time of admission, and, all dogs survived until the discharge while, in the aforementioned studies[107, 119], the majority of dogs with reduced EF% and FS% did not survive, suggesting that the standard echocardiographic indices of systolic function decrease only in case of severe cardiovascular impairment as seen in multiple organ dysfunction or failure[123]. The left ventricular EF% reduction represents a relatively late stage of systolic impairment, after the myocardium has exhausted its considerable functional reserve, moreover, EF% is highly load dependent and are insensitive to detect early or mild ventricular dysfunction, as demonstrated in dogs[132], rabbits[162], pigs[124] and humans with various diseases[126, 163–172]. In our study the Doppler derived index of systolic function PEP/ET was significantly higher (*p=0,001*) in the SIRS group (mean ± SD = 0,50 ± 0,09) than in the control group (mean ± SD = 0,41 ± 0,05) and above the reference limits[115]. This increase in the PEP/ET index was due to a reduction in ET and not to an increase in PEP. In fact, as showed in Table 7, SIRS PEP (mean ± SD = 73,94 ± 13,43) did not differ significantly (*p=0,75*) from PEP assessed in the control group (mean ± SD = 72,59 ± 10,49); instead, SIRS ET (mean ± SD = 148,71 ± 24,30) was significantly shorter (*p=0,0007*) than control group ET (mean ± SD = 174,50 ±

15,04). As previously observed[118], we found an high negative and significant correlation (Table 17) between ET and heart rate (HR) in both groups. Since the heart rate was significantly higher in SIRS group (mean ± SD = 127,82 ± 34,27) compared with the control group (mean ± SD = 105,53 ± 19,33), we concluded that the SIRS PEP/ET is higher than PEP/ET assessed in the control group because of the increased heart rate leading to a decrease of ET, and not because of a detected reduction in LV systolic function, which would have resulted in the reduction of PEP[118], not detected in the SIRS group analysed in the present study. On the basis of these results, we concluded that the standard echocardiographic parameters of systolic function such as EF%, FS% and the Doppler-derived systolic time intervals didn't reveal LV systolic dysfunction in our population of dogs with SIRS. On the contrary, the 2D Speckle Tracking indices of systolic function were able to detect early myocardial dysfunction. 2D STE is a recent echocardiographic technology that analyses myocardial motion by tracking natural acoustic reflections originating by the interaction of ultrasonic beams and the myocardium during the 2D exam. 2D STE derived Strain is a dimensionless measurement of deformation and the Global Longitudinal Peak Strain (GLPS) is the ratio of the maximal change in the myocardial longitudinal length in systole to the original length in diastole, it is viewed as a measure of systolic function representing contractility[173]. LV GLPS has been claimed to be relatively independent of load condition than EF% and FS%[174]. During systole, the LV longitudinal myofibers shorten so the longitudinal Strain is represented by a negative value, more negative values indicate better LV systolic function. In human medicine a reduction in longitudinal deformation has been found an early and accurate indicator of left ventricular dysfunction with high susceptibility to ischemia, fibrosis and hypertrophy[171, 175, 176]. In our study, the left ventricular Global Peak Longitudinal Strain of the endocardial border (LV ENDO GLPS) and the STE-derived EF% in SIRS dogs were significantly lower than those obtained in the healthy group (Table 8A and 8B, Figure 10 and 12). In fact, 2D STE-EF% calculated by the XStrain-4D™ software, fusing together 3 different

apical views, was significant (*p=0,003*) lower in the SIRS group (mean ± SD = 43,9 ± 8,4) compared to the control group (mean ± SD = 53,2 ± 8,4) and the mean LV ENDO GLPS was significantly lower (*p=0,004*) in the SIRS group (-14,60%) than the control group (-18,54%).

The LV wall comprises an endomyocardial, a mid-myocardial, and an epimyocardial layer. Normally the myocardium shows a transmural heterogeneity in myocardial blood flow, metabolism, and contraction/relaxation function[177]. Most imaging techniques consider the complete myocardial thickness in the analysis of LV function, without further distinction between different layers of the myocardium, whereas 2D-STE allows the layer-specific analysis of myocardial function as demonstrated in dogs[139] and humans[178]. Endocardial and epicardial STE variables such as displacement, velocity, Strain and Strain Rate represents, respectively the endomyocardial and epimyocardial fibres parameters of deformation during the cardiac cycle.

To the best of our knowledge no previous study has analysed the endomyocardial and epymyocardial deformation of LV in dogs with SIRS. In our study, we assessed global and regional, endomyocardial (ENDO) and epimyocardial (EPI) parameters of longitudinal contraction (displacement, velocity of displacement, Strain and Strain rate) as well as global and regional parameters of transversal (radial) ENDO and EPI contraction (displacement, velocity of displacement) assessed by the apical views. Interestingly, SIRS dogs showed a reduction in LV global and regional longitudinal peak St only in the endomyocardial fibers, in fact, no significant differences were detected in the LV epimyocardial global and regional longitudinal St between the two groups. A decrease in endomyocardial global and regional peak longitudinal St could represent more subtle changes in the myocardium of dogs with systemic inflammation, in fact the subendocardial region is the most vulnerable component of the LV wall and, therefore, the most sensitive to the presence of myocardial disease. It has been demonstrated that in healthy humans, sheep and dogs endomyocardial layer contraction is greater[139, 179, 180] and myocardial pressure and oxygen consumption are higher than in the

epimyocardial layer[181], as a consequence, higher rates of metabolic activity and oxygen extraction are found in the subendocardial region. Because of that, the production and the utilization of ATP in the endomyocardial fibers is more active but decline more easily than in the epimyocardial fibers during ischemia. It is well known that ischemic injury affects firstly the endomyocardial layer[182] and leads to a reduction in longitudinal systolic shortening in humans and dogs[183].

All these considerations led us to speculate that, in our population of dogs with SIRS, the left ventricular longitudinal endomyocardial Strain was impaired because of 2 main reasons, one is the direct negative effect of the inflammatory mediators upon endomyocardial myocite contraction and the second is the endomyocardial ischemia due to microcirculatory alterations typical of systemic inflammation. We also found a positive and significant correlation between STE-derived EF% and ENDO GPLS (Table 14), showing that STE EF% is largely due to the contraction of longitudinal endomyocardial fibres.

Our results are in agreement with the findings of recent studies in animal models of sepsis[124] and in human systemic inflammatory diseases such as sepsis[126,165,184] systemic lupus erythematosus[169], rheumatoid arthritis[172], Behcet disease[175], Kawasaki disease[185], psoriasis[186] in in which was demonstrated that GLPS decreased before to detect significant changes in standard echocardiographic-derived EF%. In human medicine GLPS has been more sensitive to EF% in detecting myocardial dysfunction also in non-inflammatory conditions such as doxorubicin-induced myocardial dysfunction[187], diabetes, hypertension[188], acute alcohol intoxication[189] and chronic kidney disease[190].

Although we found an early systolic dysfunction in dogs with SIRS, we failed to demonstrate a correlation between CRP and 2D-STE variables and between CRP and cTnI serum levels in our SIRS group, this can be due to the small number of subjects included in the study. Myocardial injury, as detected by increase in serum levels of cardiac troponins, has been frequently observed in dogs and humans with Systemic Inflammatory Response Syndrome[98] of either infectious[103] or non-infectious[59] origin. Troponins were shown to be predictors of long-term

case fatality in critically ill dogs with SIRS[97]. In the present study serum cTnI of the SIRS dogs (mean ± SD = 0,069 ± 0,071) was not significantly higher (*p=0,41*) than control group (mean ± SD = 0,054 ± 0,016) as found by Hagman et al in dogs with pyometra[109]. Probably the cTnI concentration didn't increase because of the less severity of underlying disease in our SIRS population compared to others studies. Contrary to the results of a previous study in which authors found correlation between STE-derived GLPS and cTnI serum concentration in an experimental model of sepsis induced myocardial injury rabbits[162], we failed to demonstrate a significant correlation between ENDO GPLS and cTnI serum levels.

As previously reported in dogs[138, 139], our study showed a good intra-operator within-day and between-day repeatability of STE acquisition and measurements. This result can be partially attributed to the use of a semi-automated software (2D-XStrain™ and XStrain 4D™), which helped the operator to divide the LV wall in segments.

Our study has several limitations. The small number of dogs may affect the statistical power and limit extrapolation of our findings to larger populations; also, the small number of the non-infectious SIRS (tumour and immune-mediated diseases) didn't allow comparing the STE variables between different pathologies, finally we didn't perform serial STE examination on the SIRS group, which would be useful in detects changes in LV systolic function after clinical improvement.

6. CONCLUSIONS

Increasing evidence validates the correlation between myocardial dysfunction and high mortality rates in human[191] and veterinary medicine[97, 107, 119, 192] therefore, the early detection of myocardial dysfunction in SIRS and sepsis may be crucial for predicting prognoses and facilitating early therapeutic intervention in order to reduce the duration of inflammatory illness, the severity of side effects and the mortality rate. This study has shown that 2D Speckle Tracking Echocardiography derived global and regional endomyocardial longitudinal peak Strain is more sensitive than conventional echocardiographic indices of systolic function in detecting early myocardial systolic dysfunction in dogs with Systemic Inflammatory Response Syndrome, moreover our results have demonstrated that the subendocardial region is the earlier affected part of the myocardium during inflammatory diseases. Bi-Dimensional Speckle Tracking echocardiography is a non-invasive ultrasound imaging technique, repeatable and easy to perform which could be used routinely to assess the severity and monitor the progression of myocardial dysfunction during SIRS.

REFERENCES

1. Bone RC, Sibbald WJ, Sprung CL. The ACCP-SCCM consensus conference on sepsis and organ failure. Chest 1992;101:1481–1483.

2. Ateca LB, Drobatz KJ, King LG. Organ dysfunction and mortality risk factors in severe canine bite wound trauma. J Vet Emerg Crit Care 2014;24:705–714.

3. Okano S, Yoshida M, Fukushima U, Higuchi S, Takase K, Hagio M. Usefulness of systemic inflammatory response syndrome criteria as an index for prognosis judgement. Vet Rec 2002;150:245–246.

4. Iris Kalli, Leontides LS, Mylonakis ME, Adamama-Moraitou K, Rallis T, Koutinas AF. Factors affecting the occurrence, duration of hospitalization and final outcome in canine parvovirus infection. Res Vet Sci 2010;89:174–178.

5. Pashmakova MB, Bishop M a, Steiner JM, Suchodolski JS, Barr JW. Evaluation of serum thyroid hormones in dogs with systemic inflammatory response syndrome or sepsis. J Vet Emerg Crit Care (San Antonio) 2014;24:264–271.

6. Schaefer H, Kohn B, Schweigert FJ, Raila J. Quantitative and qualitative urine protein excretion in dogs with severe inflammatory response syndrome. J Vet Intern Med 2011;25:1292–1297.

7. Bauer N, Moritz A. Coagulation response in dogs with and without systemic inflammatory response syndrome - preliminary results. Res Vet Sci 2013;94:122–131.

8. Giunti M, Troia R, Bergamini PF, Dondi F. Prospective evaluation of the acute patient physiologic and laboratory evaluation score and an extended clinicopathological profile in dogs with systemic inflammatory response syndrome. J Vet Emerg Crit Care 2014;25:n/a – n/a.

9. Min S, Kang M, Sur J, Park H. Staphylococcus pseudintermedius infection associated with nodular skin lesions and systemic inflammatory response syndrome in a dog. Can Vet J 2014;55:8–11.

10. DeClue AE, Sharp CR, Harmon M. Plasma inflammatory mediator concentrations at ICU admission in dogs with naturally developing sepsis. J Vet Intern Med 2012;26:624–630.

11. Osterbur K, Whitehead Z, Sharp CR, DeClue AE. Plasma nitrate/nitrite concentrations in dogs with naturally developing sepsis and non-infectious forms of the systemic inflammatory response syndrome. Vet Rec 2011;169:554.

12. Mrljak V, Kučer N, Kuleš J, Tvarijonaviciute A, Brkljačić M, Crnogaj M, Živičnjak T, Šmit I, Ceron JJ, Rafaj RB. Serum concentrations of eicosanoids and lipids in dogs naturally infected with Babesia canis. Vet Parasitol 2014;201:24–30.

13. Hauptman JG, Walshaw R, Olivier NB. Evaluation of the sensitivity and specificity of diagnostic criteria for sepsis in dogs. Vet Surg 1997;26:393–397.

14. Rau S, Kohn B, Richter C, Fenske N, Küchenhoff H, Hartmann K, Härtle S, Kaspers B, Hirschberger J. Plasma interleukin-6 response is predictive for severity and mortality in canine systemic inflammatory response syndrome and sepsis. Vet Clin Pathol 2007;36:253–260.

15. Feng Y, Chao W. Toll-Like Receptors and Myocardial Inflammation. Int J Inflam 2011;2011:1–21.

16. Piccinini a M, Midwood KS. DAMPening inflammation by modulating TLR signalling. Mediators Inflamm 2010;2010.

17. Doyle SL, O'Neill LAJ. Toll-like receptors: from the discovery of NFkappaB to new insights into transcriptional regulations in innate immunity. Biochem Pharmacol 2006;72:1102–1113.

18. Chong DLW, Sriskandan S. Pro-inflammatory mechanisms in sepsis. Contrib Microbiol 2011;17:86–107.

19. Yu D-H, Nho D-H, Song R-H, Kim S-H, Lee M-J, Nemzek J a, Park J. High-mobility group box 1 as a surrogate prognostic marker in dogs with systemic inflammatory response syndrome. J Vet Emerg Crit Care (San Antonio) 2010;20:298–302.

20. Neumann S, Kaup F-J, Scheulen S. Interleukin-6 (IL-6) serum concentrations in dogs with hepatitis and hepatic tumours compared with those with extra-hepatic inflammation and tumours. Comp Clin Path 2012;21:539–544.

21. Lewis DH, Chan DL, Pinheiro D, Garden OA. The immunopathology of sepsis:

Pathogen recognition, Systemic inflammation, the compensatory Anti-Inflammatory response, and Regulatory T-Cells Review Article. J Vet Intern Med 2012;26:457–482.

22. O'Brien M. The reciprocal relationship between inflammation and coagulation. Top Companion Anim Med 2012;27:46–52.

23. Otto CM, Drobatz KJ, Soter C. Endotoxemia and tumor necrosis factor activity in dogs with naturally occurring parvoviral enteritis. J Vet Intern Med 1997;11:65–70.

24. Ruaux CG, Pennington HL, Worrall S, Atwell RB. Tumor necrosis factor-alpha at presentation in 60 cases of spontaneous canine acute pancreatitis. Vet Immunol Immunopathol 1999;72:369–376.

25. Scheller J, Chalaris A, Schmidt-Arras D, Rose-John S. The pro- and anti-inflammatory properties of the cytokine interleukin-6. Biochim Biophys Acta 2011;1813:878–888.

26. Song R, Kim J, Yu D, Park C, Park J. Kinetics of IL-6 and TNF-α changes in a canine model of sepsis induced by endotoxin. Vet Immunol Immunopathol 2012;146:143–149.

27. DeClue AE, Sharp CR, Harmon M. Plasma Inflammatory Mediator Concentrations at ICU Admission in Dogs with Naturally Developing Sepsis. J Vet Intern Med 2012;26:624–630.

28. Ishida A, Ohno K, Fukushima K, Nakashima K, Takahashi M, Goto-Koshino Y, Fujino Y, Tsujimoto H. Plasma high-mobility group box 1 (HMGB1) in dogs with various diseases: comparison with C-reactive protein. J Vet Med Sci 2011;73:1127–1132.

29. De Laforcade AM, Freeman LM, Shaw SP, Brooks MB, Rozanski EA, Rush JE. Hemostatic changes in dogs with naturally occurring sepsis. J Vet Intern Med 2003;17:674–679.

30. Dircks BH, Mischke R, Schuberth H. Platet-neutrophil aggregate formation in blood samples from dogs with systemic inflammatory. Am J Vet Res 2012;73:939–945.

31. O'Brien M. The Reciprocal Relationship Between Inflammation and Coagulation. Top Companion Anim Med 2012;27:46–52.

32. Gahmberg CG, Andersson LC. Leukocyte surface origin of human alpha1-acid glycoprotein (orosomucoid). J Exp Med 1978;148:507–521.

33. Jabs WJ, Lögering BA, Gerke P, Kreft B, Wolber EM, Klinger MHF, Fricke L, Steinhoff J. The kidney as a second site of human C-reactive protein formation in vivo. Eur J Immunol 2003;33:152–161.

34. Cray C, Zaias J, Altman NH. Acute Phase Response in Animals : A Review. Comp Med 2009;59:517–526.

35. Ceciliani F, Giordano A, Spagnolo V. The systemic reaction during inflammation: the acute-phase proteins. Protein Pept Lett 2002;9:211–223.

36. Gruys E, Toussaint MJM, Niewold T a, Koopmans SJ. Acute phase reaction and acute phase proteins. J Zhejiang Univ Sci B 2005;6:1045–1056.

37. Eckersall PD, Conner JG. Bovine and canine acute phase proteins. Vet Res Commun 1988;12:169–178.

38. Yamamoto S, Tagata K, Nagahata H, Ishikawa Y, Morimatsu M, Naiki M. Isolation of canine C-reactive protein and characterization of its properties. Vet Immunol Immunopathol 1992;30:329–339.

39. Eckersall PD, Bell R. Acute phase proteins: Biomarkers of infection and inflammation in veterinary medicine. Vet J 2010;185:23–27.

40. Kuribayashi T, Shimada T, Matsumoto M, Kawato K, Honjyo T, Fukuyama M, Yamamoto Y, Yamamoto S. Determination of serum C-reactive protein (CRP) in healthy beagle dogs of various ages and pregnant beagle dogs. Exp Anim 2003;52:387–390.

41. Yamamoto S, Shida T, Okimura T, Otabe K, Honda M, Ashida Y, Furukawa E, Sarikaputi M, Naiki M. Determination of C-reactive protein in serum and plasma from healthy dogs and dogs with pneumonia by ELISA and slide reversed passive latex agglutination test. Vet Q 1994;16:74–77.

42. Caspi D, Snel FW, Batt RM, Bennett D, Rutteman GR, Hartman EG, Baltz ML, Gruys E, Pepys MB. C-reactive protein in dogs. Am J Vet Res 1987;48:919–921.

43. Yamamoto S, Shida T, Miyaji S, Santsuka H, Fujise H, Mukawa K, Furukawa E,

Nagae T, Naiki M. Changes in serum C-reactive protein levels in dogs with various disorders and surgical traumas. Vet Res Commun 1993;17:85–93.

44. Nakamura M, Takahashi M, Ohno K, Koshino A, Nakashima K, Setoguchi A, Fujino Y, Tsujimoto H. C-reactive protein concentration in dogs with various diseases. J Vet Med Sci 2008;70:127–131.

45. Christensen MB, Langhorn R, Goddard A, Andreasen EB, Moldal E, Tvarijonaviciute A, Kirpensteijn J, Jakobsen S, Persson F, Kjelgaard-hansen M. Comparison of serum amyloid A and C-reactive protein as diagnostic markers of systemic inflammation in dogs. Can Vet J 2014;55.

46. Ceron JJ, Eckersall PD, Martýnez-Subiela S. Acute phase proteins in dogs and cats: current knowledge and future perspectives. Vet Clin Pathol 2005;34:85–99.

47. Karlsson I, Wernersson S, Ambrosen a, Kindahl H, Södersten F, Wang L, Hagman R. Increased concentrations of C-reactive protein but not high-mobility group box 1 in dogs with naturally occurring sepsis. Vet Immunol Immunopathol 2013;156:64–72.

48. McClure V, Van Schoor M, Thompson P et al. Evaluation of the use of serum C-reactive protein concentration to predict outcome in puppies infected with canine parvovirus. J Am Vet Med Assoc 2013;243:361–366.

49. Viitanen SJ, Laurila HP, Lilja-Maula LI, Melamies M a, Rantala M, Rajamäki MM. Serum C-reactive protein as a diagnostic biomarker in dogs with bacterial respiratory diseases. J Vet Intern Med 2014;28:84–91.

50. Nielsen L, Toft N, Eckersall PD, Mellor DJ, Morris JS. Serum C-reactive protein concentration as an indicator of remission status in dogs with multicentric lymphoma. J Vet Intern Med 2007;21:1231–1236.

51. Tecles F, Caldin M, Zanella A, Membiela F, Tvarijonaviciute A, Subiela SM, Ceron JJ. Serum Acute Phase Protein Concentrations in Female Dogs with Mammary Tumors. J Vet Diagnostic Investig 2009;21:214–219.

52. Chase D, McLauchlan G, Eckersall PD, Pratschke J, Parkin T, Pratschke K. Acute phase protein levels in dogs with mast cell tumours and sarcomas. Vet Rec 2012;170:648.

53. Griebsch C, Arndt G, Raila J, Schweigert FJ, Kohn B. C-reactive protein

concentration in dogs with primary immune-mediated hemolytic anemia. Vet Clin Pathol 2009;38:421–425.

54. Foster JD, Sample S, Kohler R, Watson K, Muir P, Trepanier L A. Serum biomarkers of clinical and cytologic response in dogs with idiopathic immune-mediated polyarthropathy. J Vet Intern Med 2014;28:905–911.

55. Silvestrini P, Zoia A, Planellas M, Roura X, Pastor J, Cerón JJ, Caldin M. Iron status and C-reactive protein in canine leishmaniasis. J Small Anim Pract 2013;55:95–101.

56. Venco L, Bertazzolo W, Giordano G, Paltrinieri S. Evaluation of C-reactive protein as a clinical biomarker in naturally heartworm-infected dogs: A field study. Vet Parasitol 2014;206:48–54.

57. Carretón E, Morchón R, Simón F, Juste MC, Méndez JC, Montoya-Alonso JA. Cardiopulmonary and inflammatory biomarkers in the assessment of the severity of canine dirofilariosis. Vet Parasitol 2014;206:43–47.

58. Mansfield CS, James FE, Robertson ID. Development of a clinical severity index for dogs with acute pancreatitis. J Am Vet Med Assoc 2008;233:936–944.

59. Langhorn R, Persson F, Blad B, Goddard A, Schoeman JP, Willesen JL, Tarnow I, Kjelgaard-Hansen M. Myocardial injury in dogs with snake envenomation and its relation to systemic inflammation. J Vet Emerg Crit Care 2013;24:174–181.

60. Ulutas PA, Musal B, Kiral F, Bildik A. Acute phase protein levels in pregnancy and oestrus cycle in bitches. Res Vet Sci 2009;86:373–376.

61. Gebhardt C, Hirschberger J. Use of C-reactive protein to predict outcome in dogs with systemic inflammatory response syndrome or sepsis. J Vet Emerg Crit Care 2009;19:450–458.

62. Barie PS, Hydo LJ, Pieracci FM, Shou J, Eachempati SR. Multiple organ dysfunction syndrome in critical surgical illness. Surg Infect (Larchmt) 2009;10:369–377.

63. Balk RA. Pathogenesis and management of multiple organ dysfunction or failure in severe sepsis and septic shock. Crit Care Clin 2000;16:337–352, vii.

64. Kenney EM, Rozanski E a, Rush JE, DeLaforcade-Buress AM, Berg JR, Silverstein DC, Montealegre CD, Jutkowitz LA, Adamantos S, Ovbey DH, Boysen SR, Shaw SP. Association between outcome and organ system dysfunction in dogs with sepsis: 114 cases (2003-2007). J Am Vet Med Assoc 2010;236:83–87.

65. Abraham E. Nuclear factor-kappaB and its role in sepsis-associated organ failure. J Infect Dis 2003;187 Suppl:S364–S369.

66. Schulze-Osthoff K, Bakker AC, Vanhaesebroeck B, Beyaert R, Jacob WA, Fiers W. Cytotoxic activity of tumor necrosis factor is mediated by early damage of mitochondrial functions. Evidence for the involvement of mitochondrial radical generation. J Biol Chem 1992;267:5317–5323.

67. Supinski GS, Callahan LA. Polyethylene glycol-superoxide dismutase prevents endotoxin-induced cardiac dysfunction. Am J Respir Crit Care Med 2006;173:1240–1247.

68. Suliman HB, Carraway MS, Piantadosi CA. Postlipopolysaccharide oxidative damage of mitochondrial DNA. Am J Respir Crit Care Med 2003;167:570–579.

69. Brealey D, Karyampudi S, Jacques TS, Novelli M, Stidwill R, Taylor V, Smolenski RT, Singer M. Mitochondrial dysfunction in a long-term rodent model of sepsis and organ failure. Am J Physiol Regul Integr Comp Physiol 2004;286:R491–R497.

70. Klabunde RE. Cardiovascular Physiology Concepts. Heart Fail 2005:235.

71. Parrillo JE, Parker MM, Natanson C, Suffredini AF, Danner RL, Cunnion RE, Ognibene FP. Septic shock in humans. Advances in the understanding of pathogenesis, cardiovascular dysfunction, and therapy. Ann Intern Med 1990;113:227–242.

72. Hoesel LM, Niederbichler AD, Ward PA. Complement-related molecular events in sepsis leading to heart failure. Mol Immunol 2007;44:95–102.

73. Werdan K, Schmidt H, Ebelt H, Zorn-Pauly K, Koidl B, Hoke RS, Heinroth K, Müller-Werdan U. Impaired regulation of cardiac function in sepsis, SIRS, and MODS. Can J Physiol Pharmacol 2009;87:266–274.

74. Parrillo JE. The cardiovascular pathophysiology of sepsis. Annu Rev Med 1989;40:469–485.

75. Wiggers CJ. Myocardial depression in shock; a survey of cardiodynamic studies. Am Heart J 1947;33:633–650.

76. Lefer AM. Mechanisms of cardiodepression in endotoxin shock. Circ Shock Suppl 1979;1:1–8.

77. Parrillo JE, Burch C, Shelhamer JH, Parker MM, Natanson C, Schuette W. A circulating myocardial depressant substance in humans with septic shock. Septic shock patients with a reduced ejection fraction have a circulating factor that depresses in vitro myocardial cell performance. J Clin Invest 1985;76:1539–1553.

78. Price S, Anning PB, Mitchell JA, Evans TW. Myocardial dysfunction in sepsis: mechanisms and therapeutic implications. Eur Heart J 1999;20:715–724.

79. Clowes GH, Vucinic M, Weidner MG. Circulatory and metabolic alterations associated with survival or death in peritonitis: clinical analysis of 25 cases. Ann Surg 1966;163:866–885.

80. Cunnion RE, Schaer GL, Parker MM, Natanson C, Parrillo JE. The coronary circulation in human septic shock. Circulation 1986;73:637–644.

81. Snell RJ, Parrillo JE. Cardiovascular dysfunction in septic shock. Chest 1991;99:1000–1009.

82. Stein B, Frank P, Schmitz W, Scholz H, Thoenes M. Endotoxin and cytokines induce direct cardiodepressive effects in mammalian cardiomyocytes via induction of nitric oxide synthase. J Mol Cell Cardiol 1996;28:1631–1639.

83. Pathan N, Hemingway CA, Alizadeh AA, Stephens AC, Boldrick JC, Oragui EE, McCabe C, Welch SB, Whitney A, O'Gara P, Nadel S, Relman DA, Harding SE, Levin M. Role of interleukin 6 in myocardial dysfunction of meningococcal septic shock. Lancet 2004;363:203–209.

84. Lew WY, Yasuda S, Yuan T, Hammond HK. Endotoxin-induced cardiac depression is associated with decreased cardiac dihydropyridine receptors in rabbits. J Mol Cell Cardiol 1996;28:1367–1371.

85. Zhong J, Hwang TC, Adams HR, Rubin LJ. Reduced L-type calcium current in ventricular myocytes from endotoxemic guinea pigs. Am J Physiol

1997;273:H2312–H2324.

86. Rigby SL, Hofmann P A, Zhong J, Adams HR, Rubin LJ. Endotoxemia-induced myocardial dysfunction is not associated with changes in myofilament Ca2+ responsiveness. Am J Physiol 1998;274:H580–H590.

87. Stengl M, Bartak F, Sykora R, Chvojka J, Benes J, Krouzecky A, Novak I, Sviglerova J, Kuncova J, Matejovic M. Reduced L-type calcium current in ventricular myocytes from pigs with hyperdynamic septic shock. Crit Care Med 2010;38:579–587.

88. Chopra M. Distinct cardiodynamic and molecular characteristics during early and late stages of sepsis-induced myocardial dysfunction. Life Sci 2007;81:306–316.

89. Ren J, Wu S. A burning issue: do sepsis and systemic inflammatory response syndrome (SIRS) directly contribute to cardiac dysfunction? Front Biosci 2006;11:15–22.

90. Merx MW, Weber C. Sepsis and the heart. Circulation 2007;116:793–802.

91. Massey C V, Kohout TA, Gaa ST, Lederer WJ, Rogers TB. Molecular and cellular actions of platelet-activating factor in rat heart cells. J Clin Invest 1991;88:2106–2116.

92. Silverman HJ, Penaranda R, Orens JB, Lee NH. Impaired beta-adrenergic receptor stimulation of cyclic adenosine monophosphate in human septic shock: association with myocardial hyporesponsiveness to catecholamines. Crit Care Med 1993;21:31–39.

93. Zorn-Pauly K, Pelzmann B, Lang P, Mächler H, Schmidt H, Ebelt H, Werdan K, Koidl B, Müller-Werdan U. Endotoxin impairs the human pacemaker current If. Shock 2007;28:655–661.

94. Walley KR, Becker CJ, Hogan R a, Teplinsky K, Wood LD. Progressive hypoxemia limits left ventricular oxygen consumption and contractility. Circ Res 1988;63:849–859.

95. Steenbergen C, Deleeuw G, Rich T, Williamson JR. Effects of acidosis and ischemia on contractility and intracellular pH of rat heart. Circ Res 1977;41:849–858.

96. Ammann P, Fehr T, Minder E, Günter C, Bertel O. Elevation of troponin I in sepsis and septic shock. Intensive Care Med 2001;27:965–969.

97. Langhorn R, Oyama M a, King LG, Machen MC, Trafny DJ, Thawley V, Willesen JL, Tarnow I, Kjelgaard-Hansen M. Prognostic importance of myocardial injury in critically ill dogs with systemic inflammation. J Vet Intern Med 2013;27:895–903.

98. Hamacher L, D Orfelt R, Wess G. Serum Cardiac Troponin I Concentrations in Dogs with Systemic Inflammatory Response Syndrome 2015:164–170.

99. Wu A. HB, Jialal I. How specific is cardiac troponin? Am J Clin Pathol 2000;114:509–511.

100. Wells SM, Sleeper M. Cardiac troponins. J Vet Emerg Crit Care 2008;18:235–245.

101. Cummins B, Cummins P. Cardiac specific troponin-I release in canine experimental myocardial infarction: development of a sensitive enzyme-linked immunoassay. J Mol Cell Cardiol 1987;19:999–1010.

102. Langhorn R, Persson F, Ablad B, Goddard A, Schoeman JP, Willesen JL, Tarnow I, Kjelgaard-Hansen M. Myocardial injury in dogs with snake envenomation and its relation to systemic inflammation. J Vet Emerg Crit Care (San Antonio) 2014;24:174–181.

103. Diniz PPVP, de Morais HS a, Breitschwerdt EB, Schwartz DS. Serum cardiac troponin I concentration in dogs with ehrlichiosis. J Vet Intern Med 2008;22:1136–1143.

104. Burgener IA, Kovacevic A, Mauldin GN, Lombard CW. Cardiac troponins an indicators of acute Myocardial damage in Dogs. J Vet Intern Med 2006;20:277–283.

105. Lobetti R, Kirberger R, Keller N, Kettner F, Dvir E. NT-ProBNP and cardiac troponin I in virulent canine babesiosis. Vet Parasitol 2012;190:333–339.

106. Pelander L, Hagman R, Häggström J. Concentrations of cardiac Troponin I before and after ovariohysterectomy in 46 female dogs with pyometra. Acta Vet Scand 2008;50:35.

107. Kocaturk M, Martinez S, Eralp O, Tvarijonaviciute A, Ceron J, Yilmaz Z. Tei index (myocardial performance index) and cardiac biomarkers in dogs with parvoviral enteritis. Res Vet Sci 2012;92:24–29.

108. Silvestrini P, Piviani M, Alberola J, Rodríguez-Cortés A, Planellas M, Roura X, O'Brien PJ, Pastor J. Serum cardiac troponin I concentrations in dogs with leishmaniasis: correlation with age and clinicopathologic abnormalities. Vet Clin Pathol 2012;41:568–574.

109. Hagman R, Lagerstedt A-S, Fransson B a, Bergström A, Häggström J. Cardiac troponin I levels in canine pyometra. Acta Vet Scand 2007;49:6.

110. Mason DJ, O'Grady M, Woods JP, McDonell W. Assessment of lithium dilution cardiac output as a technique for measurement of cardiac output in dogs. Am J Vet Res 2001;62:1255–1261.

111. Butler AL, Campbell VL, Wagner AE, Sedacca CD, Hackett TB. Lithium dilution cardiac output and oxygen delivery in conscious dogs with systemic inflammatory response syndrome. J Vet Emerg Crit Care 2008;18:246–257.

112. Gommeren K, Desmas I, Garcia A, Clercx C, Mc Entee K, Peeters D. Cardiac ultrasound in canine emergencies with a systemic inflammatory response syndrome. Oral Research Communications of the 22 nd ECVIM-CA Congress, Maastricht, Netherlands, 6th to 8th September 2012. J Vet Intern Med 2012;26:1505–1538.

113. Chetbul V, Bussadori C, De Madron E. Clinical echocardiography of the dog and cat. 2015.

114. Brown DJ, Rush JE, MacGregor J, Ross JN, Brewer B, Rand WM. M-mode echocardiographic ratio indices in normal dogs, cats, and horses: a novel quantitative method. J Vet Intern Med 2003;17:653–662.

115. Dukes-McEwan J, Borgarelli M, Tidholm A, Vollmar AC, Häggström J. Proposed Guidelines for the Diagnosis of Canine Idiopathic Dilated Cardiomyopathy 2003;5.

116. O'Sullivan ML, O'Grady MR, Minors SL. Assessment of diastolic function by Doppler echocardiography in normal Doberman Pinschers and Doberman Pinschers with dilated cardiomyopathy. J Vet Intern Med 2007;21:81–91.

117. Serres F, Chetboul V, Tissier R, Poujol L, Gouni V, Carlos Sampedrano C,

Pouchelon JL. Comparison of 3 ultrasound methods for quantifying left ventricular systolic function: correlation with disease severity and prognostic value in dogs with mitral valve disease. J Vet Intern Med 2008;22:566–577.

118. Atkins C, Snyder P. Systolic Time Intervals and Their Derivates for evaluation of Cardiac Function. J Vet Intern Med 1992.

119. Nelson OL, Thompson PA. Cardiovascular dysfunction in dogs associated with critical illnesses. J Am Anim Hosp Assoc 2006;42:344–349.

120. Dickinson AE, Rozanski EA, Rush JE. Reversible myocardial depression associated with sepsis in a dog. J Vet Intern Med 2007;21:1117–1120.

121. Kocatürk M, Salci H, Yilmaz Z, Bayram A. S, Koch J. Pre-and post-operative cardiac evaluation of dogs undergoing lobectomy and pneumonectomy. J Vet Sci 2010;11:257–264.

122. Tei C. New non-invasive index for combined systolic and diastolic ventricular function. J Cardiol 1995;26:135–136.

123. Osterbur K, Mann FA, Kuroki K, DeClue A. Multiple Organ Dysfunction Syndrome in Humans and Animals. J Vet Intern Med 2014:1141–1151.

124. Hestenes SM, Halvorsen PS, Skulstad H, Remme EW, Espinoza A, Hyler S, Bugge JF, Fosse E, Nielsen EW, Edvardsen T. Advantages of Strain Echocardiography in Assessment of Myocardial Function in Severe Sepsis: An Experimental Study. Crit Care Med 2014;42:432–440.

125. Pulido JN, Afessa B, Masaki M, Yuasa T, Gillespie S, Herasevich V, Brown DR, Oh JK. Clinical spectrum, frequency, and significance of myocardial dysfunction in severe sepsis and septic shock. Mayo Clin Proc 2012;87:620–628.

126. Dalla K, Hallman C, Bech-Hanssen O, Haney M, Ricksten S-E. Strain echocardiography identifies impaired longitudinal systolic function in patients with septic shock and preserved ejection fraction. Cardiovasc Ultrasound 2015;13:30.

127. Borlaug BA, Paulus WJ. Heart failure with preserved ejection fraction: Pathophysiology, diagnosis, and treatment. Eur Heart J 2011;32:670–679.

128. Blessberger H, Binder T. Two dimensional speckle tracking echocardiography:

basic principles. Heart 2010;96:716–722.

129. Chetboul V. Advanced techniques in echocardiography in small animals. Vet Clin North Am Small Anim Pract 2010;40:529–543.

130. Mondillo S, Galderisi M, Mele D, Cameli M, Lomoriello VS, Ballo P, Muraru D, Losi M, Agricola E, Buralli S, Sciomer S, Nistri S, Badano L. Speckle-Tracking Echocardiography. J Ultrasound Med 2011:71–83.

131. Brown J, Jenkins C, Marwick TH. Use of myocardial strain to assess global left ventricular function: A comparison with cardiac magnetic resonance and 3-dimensional echocardiography. Am Heart J 2009;157.

132. Culwell NM, Bonagura JD, Schober KE. Comparison of echocardiographic indices of myocardial strain with invasive measurements in anesthetized healthy dogs. Am J Vet Res 2011;72.

133. Amundsen BH, Helle-Valle T, Edvardsen T, Torp H, Crosby J, Lyseggen E, Støylen A, Ihlen H, Lima J a C, Smiseth O A, Slørdahl S A. Noninvasive myocardial strain measurement by speckle tracking echocardiography: Validation against sonomicrometry and tagged magnetic resonance imaging. J Am Coll Cardiol 2006;47:789–793.

134. Lima J A, Jeremy R, Guier W, Bouton S, Zerhouni E A, McVeigh E, Buchalter MB, Weisfeldt ML, Shapiro EP, Weiss JL. Accurate systolic wall thickening by nuclear magnetic resonance imaging with tissue tagging: correlation with sonomicrometers in normal and ischemic myocardium. J Am Coll Cardiol 1993;21:1741–1751.

135. Rajapakshage W, Kumara B, Murakami M. Repeatability and reproducibility of measurements obtained via 2D STEof thw LA and time-LA-area curve analysis in healthy dogs. Am J Vet Res 2013;74:2–7.

136. Chetboul V, Serres F, Gouni V, Tissier R, Pouchelon J-L. Radial strain and strain rate by two-dimensional speckle tracking echocardiography and the tissue velocity based technique in the dog. J Vet Cardiol 2007;9:69–81.

137. Chetboul V, Serres F, Gouni V, Tissier R, Pouchelon JL. Noninvasive Assessment of Systolic Left Ventricular Torsion by 2-Dimensional Spekle Tracking Imaging in the Awake Dog: Repetibility, Reproducibility, and Comparison with Tissue Doppler Imaging Variables. J Vet Intern Med 2008:342–350.

138. Wess G, Keller LJM, Klausnitzer M, Killich M, Hartmann K. Comparison of longitudinal myocardial tissue velocity, strain, and strain rate measured by two-dimensional speckle tracking and by color tissue Doppler imaging in healthy dogs. J Vet Cardiol 2011;13:31–43.

139. Carnabuci C, Hanås S, Ljungvall I, Tidholm A, Bussadori C, Häggström J, Höglund K. Assessment of cardiac function using global and regional left ventricular endomyocardial and epimyocardial peak systolic strain and strain rate in healthy Labrador retriever dogs. Res Vet Sci 2013;95:241–248.

140. Suzuki R, Matsumoto H, Teshima T, Koyama H. Effect of age on myocardial function assessed by two-dimensional speckle-tracking echocardiography in healthy beagle dogs. J Vet Cardiol 2013;15:243–252.

141. Suzuki R, Matsumoto H, Teshima T, Koyama H. Influence of heart rate on myocardial function using two-dimensional speckle-tracking echocardiography in healthy dogs. J Vet Cardiol 2013;15:139–146.

142. Wong VM, Kidney B A, Snead ECR, Myers SL, Jackson ML. Serum C-reactive protein concentrations in healthy Miniature Schnauzer dogs. Vet Clin Pathol 2011;40:380–383.

143. Muzzi R AL, de Araújo RB, Muzzi L AL, Pena JL, Silva EF. Regurgitant jet area by Doppler color flow mapping: quantitative assessment of mitral regurgitation severity in dogs. J Vet Cardiol 2003;5:33–38.

144. Gouni V, Serres FJ, Pouchelon J-L, Tissier R, Lefebvre HP, Nicolle AP, Sampedrano CC, Chetboul V. Quantification of mitral valve regurgitation in dogs with degenerative mitral valve disease by use of the proximal isovelocity surface area method. J Am Vet Med Assoc 2007;231:399–406.

145. Sykes JE, Hartmann K, Lunn KF, Moore GE, Stoddard R A, Goldstein RE. ACVIM Consensus Statement. J Vet Intern Med 2011;19:1–13.

146. Kellihan HB, Stepien RL. Pulmonary hypertension in dogs: diagnosis and therapy. Vet Clin North Am Small Anim Pract 2010;40:623–641.

147. Serres FJ, Chetboul V, Tissier R, Sampedrano CC, Gouni V, Nicolle AP. Doppler echocardiography-derived evidence of pulmonary arterial hypertension in dogs with degenerative mitral valve disease : 86 cases (2001 – 2005). JAVMA 2006;229:1772–1778.

148. Bodey AR, Sansom J. Epidemiological study of blood pressure in domestic cats. J Small Anim Pract 1998;39:567–573.

149. Sleeper MM, Clifford CA, Laster LL. Cardiac troponin 1 in the normal dog and cat. J Vet Intern Med 2001;15:501–503.

150. Lang RM, Bierig M, Devereux RB, Flachskampf FA, Foster E, Pellikka PA, Picard MH, Roman MJ, Seward J, Shanewise J, Solomon S, Spencer KT, St. John Sutton M, Stewart W. Recommendations for chamber quantification. Eur J Echocardiogr 2006;7:79–108.

151. Sahn DJ, DeMaria A, Kisslo J, Weyman A. Recommendations regarding quantitation in M-mode echocardiography: results of a survey of echocardiographic measurements. Circulation 1978;58:1072–1083.

152. Cornell CC, Kittleson MD, Della Torre P, Häggström J, Lombard CW, Pedersen HD, Vollmar A, Wey A. Allometric scaling of M-mode cardiac measurements in normal adult dogs. J Vet Intern Med 2004;18:311–321.

153. Teichholz LE, Kreulen T, Herman M V, Gorlin R. Problems in echocardiographic volume determinations: echocardiographic-angiographic correlations in the presence of absence of asynergy. Am J Cardiol 1976;37:7–11.

154. Wess G, Mäurer J, Simak J, Hartmann K. Use of Simpson's method of disc to detect early echocardiographic changes in Doberman Pinschers with dilated cardiomyopathy. J Vet Intern Med 2010;24:1069–1076.

155. Burwash IG, Otto CM, Pearlman AS. Use of Doppler-derived left ventricular time intervals for noninvasive assessment of systolic function. Am J Cardiol 1993;72:1331–1333.

156. Mattoon J, Nyland TG. Small Animal Diagnostic Ultrasound, third edition. 2015.

157. Voigt J-U, Pedrizzetti G, Lysyansky P, Marwick TH, Houle H, Baumann R, Pedri S, Ito Y, Abe Y, Metz S, Song JH, Hamilton J, Sengupta PP, Kolias TJ, d'Hooge J, Aurigemma GP, Thomas JD, Badano LP. Definitions for a Common Standard for 2D Speckle Tracking Echocardiography: Consensus Document of the EACVI/ASE/Industry Task Force to Standardize Deformation Imaging. J Am Soc Echocardiogr 2015;28:183–193.

158. Schwarzwald CC, Schober KE, Berli ASJ, Bonagura JD. Left ventricular radial and circumferential wall motion analysis in horses using strain, strain rate, and

displacement by 2D speckle tracking. J Vet Intern Med 2009;23:890–900.

159. Mukaka MM. Statistics corner: A guide to appropriate use of correlation coefficient in medical research. Malawi Med J 2012;24:69–71.

160. Baumwart RD, Meurs KM, Bonagura JD. Tei index of myocardial performance applied to the right ventricle in normal dogs. J Vet Intern Med 2005;19:828–832.

161. Parker MM, Shelhamer JH, Bacharach SL, Green M V, Natanson C, Frederick TM, Damske BA, Parrillo JE. Profound but reversible myocardial depression in patients with septic shock. Ann Intern Med 1984;100:483–490.

162. Li T, Liu J, Du W, Wang X, Chen Z, Zhang L. Induced Early Systolic Myocardial Dysfunction. Eur Rev Med Pharmacol Sci 2014;18:3105–3114.

163. Abdel-Salam Z, Khalifa M, Ayoub A, Hamdy A, Nammas W. Early changes in longitudinal deformation indices in young asymptomatic patients with type 1 diabetes mellitus: assessment by speckle-tracking echocardiography. Minerva Cardioangiol 2014.

164. Barbosa MM, Rocha MOC, Vidigal DF, de Carvalho Bicalho Carneiro R, Araújo RD, Palma MC, de Barros MVL, Nunes MCP. Early Detection of Left Ventricular Contractility Abnormalities by Two-Dimensional Speckle Tracking Strain in Chagas' Disease. Echocardiography 2014;31:623–630.

165. Basu S, Frank LH, Fenton KE, Sable CA, Levy RJ, Berger JT. Two-dimensional speckle tracking imaging detects impaired myocardial performance in children with septic shock, not recognized by conventional echocardiography. Pediatr Crit Care Med 2012;13:259–264.

166. Bellavia D, Pellikka P A., Abraham TP, Al-Zahrani GB, Dispenzieri A, Oh JK, Bailey KR, Wood CM, Lacy MQ, Miyazaki C, Miller F A. Evidence of Impaired Left Ventricular Systolic Function by Doppler Myocardial Imaging in Patients With Systemic Amyloidosis and No Evidence of Cardiac Involvement by Standard Two-Dimensional and Doppler Echocardiography. Am J Cardiol 2008;101:1039–1045.

167. Di Bella G, Minutoli F, Pingitore A, Zito C, Mazzeo A, Aquaro GD, Di Leo R, Recupero A, Stancanelli C, Baldari S, Vita G, Carerj S. Endocardial and epicardial deformations in cardiac amyloidosis and hypertrophic cardiomyopathy. Circ J 2011;75:1200–1208.

168. Hare JL, Brown JK, Leano R, Jenkins C, Woodward N, Marwick TH. Use of myocardial deformation imaging to detect preclinical myocardial dysfunction before conventional measures in patients undergoing breast cancer treatment with trastuzumab. Am Heart J 2009;158:294–301.

169. Leal GN, Silva KF, Lianza AC, Giacomin MF, Andrade JL, Kozu K, Bonfá E. Subclinical left ventricular dysfunction in childhood-onset systemic lupus erythematosus : a two-dimensional speckle-tracking echocardiographic study erythematosus : a two-dimensional speckle-tracking echocardiographic. Scand J Rheumatol 2015;9742.

170. Liu Y-W, Tsai W-C, Su C-T, Lin C-C, Chen J-H. Evidence of Left Ventricular Systolic Dysfunction Detected by Automated Function Imaging in Patients With Heart Failure and Preserved Left Ventricular Ejection Fraction. J Card Fail 2009;15:782–789.

171. Miyoshi T, Tanaka H, Kaneko A, Tatsumi K, Matsumoto K, Minami H, Kawai H, Hirata K. Left Ventricular Endocardial Dysfunction in Patients with Preserved Ejection Fraction after Receiving Anthracycline. Echocardiography 2013:n/a – n/a.

172. Sitia S, Tomasoni L, Cicala S, Atzeni F, Ricci C, Gaeta M, Sarzi-Puttini P, Turiel M. Detection of preclinical impairment of myocardial function in rheumatoid arthritis patients with short disease duration by speckle tracking echocardiography. Int J Cardiol 2012;160:8–14.

173. De Geer L, Engvall J, Oscarsson A. Strain echocardiography in septic shock – a comparison with systolic and diastolic function parameters, cardiac biomarkers and outcome. Crit Care 2015;19:122.

174. Geyer H, Caracciolo G, Abe H, Wilansky S, Carerj S, Gentile F, Nesser HJ, Khandheria B, Narula J, Sengupta PP. Assessment of Myocardial Mechanics Using Speckle Tracking Echocardiography: Fundamentals and Clinical Applications. J Am Soc Echocardiogr 2010;23:351–369.

175. Yagmur J, Sener S, Acikgoz N, Cansel M, Ermis N, Karincaoglu Y, Tasolar H, Karakus Y, Pekdemir H, Ozdemir R. Subclinical left ventricular dysfunction in Behcet's disease assessed by two-dimensional speckle tracking echocardiography. Eur J Echocardiogr 2011;12:536–541.

176. Ng ACT, Delgado V, Bertini M, van der Meer RW, Rijzewijk LJ, Shanks M, Nucifora G, Smit JWA, Diamant M, Romijn JA, de Roos A, Leung DY, Lamb

HJ, Bax JJ. Findings from Left Ventricular Strain and Strain Rate Imaging in Asymptomatic Patients With Type 2 Diabetes Mellitus. Am J Cardiol 2009;104:1398–1401.

177. Kuwada Y, Takenaka K. [Transmural heterogeneity of the left ventricular wall: subendocardial layer and subepicardial layer]. J Cardiol 2000;35:205–218.

178. Adamu U, Schmitz F, Becker M, Kelm M, Hoffmann R. Advanced speckle tracking echocardiography allowing a three-myocardial layer-specific analysis of deformation parameters. Eur J Echocardiogr 2009;10:303–308.

179. Ishizu T, Seo Y, Enomoto Y, Sugimori H, Yamamoto M, MacHino T, Kawamura R, Aonuma K. Experimental validation of left ventricular transmural strain gradient with echocardiographic two-dimensional speckle tracking imaging. Eur J Echocardiogr 2010;11:377–385.

180. Zhang Q, Fang F, Liang YJ, Xie JM, Wen YY, Yip GWK, Lam YY, Chan JYS, Fung JWH, Yu CM. A novel multi-layer approach of measuring myocardial strain and torsion by 2D speckle tracking imaging in normal subjects and patients with heart diseases. Int J Cardiol 2011;147:32–37.

181. Weiss HR, Neubauer J A, Lipp J A, Sinha AK. Quantitative determination of regional oxygen consumption in the dog heart. Circ Res 1978;42:394–401.

182. Reimer KA, Jennings RB. The "wavefront phenomenon" of myocardial ischemic cell death. II. Transmural progression of necrosis within the framework of ischemic bed size (myocardium at risk) and collateral flow. Lab Invest 1979;40:633–644.

183. Ono S, Waldman LK, Yamashita H, Covell JW, Ross J. Effect of Coronary Artery Reperfusion on Transmural Myocardial Remodeling in Dogs. Circulation 1995;91:1143–1153.

184. Chang W-T, Lee W-H, Lee W-T, Chen P-S, Su Y-R, Liu P-Y, Liu Y-W, Tsai W-C. Left ventricular global longitudinal strain is independently associated with mortality in septic shock patients. Intensive Care Med 2015;41:1791–1799.

185. Yu JJ, Choi HS, Kim YB, Son JS, Kim Y-H, Ko J-K, Park I-S. Analyses of Left Ventricular Myocardial Deformation by Speckle-Tracking Imaging During the Acute Phase of Kawasaki Disease. Pediatr Cardiol 2010;31:807–812.

186. Bülbül Şen B, Ekiz Ö, Rifaioğlu EN, Büyükkaya E, Karakaş MF, Büyükkaya Ş, Bilen P, Akçay AB, Kurt M, Şen N. Assessment of subclinical left ventricular dysfunction in patients with psoriasis by speckle tracking echocardiography: A Speckle Tracking Study. Int J Dermatol 2015:n/a – n/a.

187. Al-Biltagi M, Abd Rab Elrasoul Tolba O, El-Shanshory MR, Abd El-Aziz El-Shitany N, El-Sayed El-Hawary E. Strain Echocardiography in Early Detection of Doxorubicin-Induced Left Ventricular Dysfunction in Children with Acute Lymphoblastic Leukemia. ISRN Pediatr 2012;2012:1–9.

188. Imbalzano E, Zito C, Carerj S, Oreto G, Mandraffino G, Cusmà-Piccione M, Di Bella G, Saitta C, Saitta A. Left ventricular function in hypertension: new insight by speckle tracking echocardiography. Echocardiography 2011;28:649–657.

189. Reant P, Chasseriaud W, Pillois X, Dijos M, Arsac F, Roudaut R, Lafitte S. Early Detection of Left Ventricular Systolic Dysfunction Using Two-Dimensional Speckle Tracking Strain Evaluation in Healthy Subjects after Acute Alcohol Intoxication. Echocardiography 2012;29:927–932.

190. Yan P, Li H, Hao C, Shi H, Gu Y, Huang G, Chen J. 2D-Speckle Tracking Echocardiography Contributes to Early Identification of Impaired Left Ventricular Myocardial Function in Patients with Chronic Kidney Disease. Nephron Clin Pract 2011;118:232–240.

191. Krishnagopalan S, Kumar A, Parrillo JE, Kumar A. Myocardial dysfunction in the patient with sepsis. Curr Opin Crit Care 2002;8:376–388.

192. Borde L, Amory H, Grulke S, Leroux A A, Houben RM, Detilleux J, Sandersen CC. Prognostic value of echocardiographic and Doppler parameters in horses admitted for colic complicated by systemic inflammatory response syndrome. J Vet Emerg Crit Care (San Antonio) 2014;24:302–310.